Russian Chemical Reviews **66** (1) 53 – 72 (1997) © 1997 Russian Academy of Sciences and Turpion Ltd

UDC 539.23 : 541.4 : 621.793.182

The synthesis and properties of interstitial phase films

R A Andrievskii

Contents

I.	Introduction	53
II.	Preparation	53
III.	Composition, structure, defects, and eletronic structure	56
IV.	Properties	61
V.	Conclusion	68

Abstract. The methods of synthesis of interstitial phase films (transition metal carbide, nitride, boride, and hydride films) are described. Different versions of their chemical and physical deposition from the gas phase are compared and discussed. The available information about the structures, electronic structures, and physicochemical properties of the films (including alloyed and multilayer films) is surveyed and analysed. The bibliography includes 225 references.

I. Introduction

The term 'interstitial phases' (IP) (or interstitial alloys, interstitial compounds, and Hagg's phases) appeared more than 60 years ago in studies of the structures of the phases in transition metal – light nonmetallic element (hydrogen, nitrogen, boron, carbon, etc.) systems. Hagg [1] put forward the hypothesis that the small atoms of the light elements are inserted in the interatomic sites within typical close-packed metallic structures: face-centred cubic (FCC), hexagonal close-packed (HCP), and body-centred cubic (BCC).

The structures of typical IP of the NaCl type, in which the octahedral positions in the metallic FCC sublattice are occupied by carbon or nitrogen atoms, and of the CaF_2 type, in which the hydrogen atoms are located in tetrahedral positions of the FCC lattice, are well known from the results of neutron diffraction studies.[2] The structures of the borides are somewhat more complex in most cases than those of the hydrides, carbides, and nitrides, but the familiar simple relations, proposed by Hagg and based on a purely geometrical approach, proved suitable only for stoichiometric phases. Deviation from stoichiometry led in the vast majority of cases to the ordering of the nonmetallic sublattice and the formation of IP with a complex structure, the metallic sublattice of which was no longer in any way characterised by simple FCC, HCP, or BCC type packing. For this reason, as has been emphasised in the monograph of the present author and Umanskii,[2] the term 'interstitial phases' is mainly of historical significance. At the present time the IP include Group III – VI transition metal hydrides, nitrides, carbides, and borides with metal-like properties, as well as certain monoxides (for example, TiO). A series of monographs (see, for example, Refs 2 – 21) and a multiplicity of communications have been published in collections and numerous periodicals devoted to the problems of the preparation, properties and applications of IP. However, questions concerning films have been described in the monograph literature on a very limited scale — so far as we are aware, only in a single monograph.[7] This situation is due to the fact that IP films began to be actively investigated only during the last 10 – 15 years after the development of an effective method for their preparation by physical deposition from the gas phase (the so called PVD technology), although chemical deposition from the gas phase (the CVD technology) had long been known. The extensive application of such films in the tool industry and in electronics stimulated the study of the characteristic features of their synthesis and properties. As regards the number of publications, titanium nitride is the undoubted leader. In this connection, one should note the reviews [22 – 28] and certain monographs on films and coatings.[29 – 31] The available information on nitride, boride, carbide, and hydride films is scattered in the periodical literature and needs to be surveyed. We may also note that this problem appears of current interest also in connection with the development of studies on IP-based nanocrystalline materials.[32, 33]

R A Andrievskii Institute of New Chemical Problems, Russian Academy of Sciences, 142432 Chernogolovka, Moscow Region, Russian Federation. Fax (7-95) 742 00 04. Tel (7-095) 524 50 24. E-mail ara@incp.ac.ru

Received 18 September 1996
Uspekhi Khimii **66** (1) 57 – 77 (1997); translated by A K Grzybowski

II. Preparation

We shall consider films with a thickness up to several micrometers. Thicker films and coatings will not as a rule be analysed. Table 1 presents the principal methods of preparation of IP films. The classification presented is arbitrary because, for example, many physical methods include chemical reactions and chemical procedures have been stimulated by physical influences.[32] The table includes only the principal methods of synthesis (vaporisation and condensation processes in an inert medium or in the reaction medium are usually implied). Nitride films can be obtained by virtually all methods, while hydride films can be prepared only by the low-temperature methods in view of the considerable dissociation pressures of the hydrides. The carbide and boride films occupy an intermediate position.

1. Physical methods

a. Thermal evaporation

In connection with the high melting points of the majority of carbides, nitrides, and borides, the processes involving evaporation by resistive or radiation-induced heating are used compara-

Table 1. Principal methods of preparation of IP films.

Method	Principal varieties	Compound
Physical methods		
Thermal evaporation	Activated reactive evaporation	Nitrides and carbides
	Electron-beam heating	Borides and carbides
	Laser treatment	Nitrides and carbides
Ion plating	Ion arc sputtering	Nitrides and carbides
	Magnetron sputtering	Nitrides, borides, carbides and hydrides
	Ion-beam treatment; implantation	Nitrides and borides
Chemical methods		
Deposition from gas phase	Plasma-associated and plasma-activated CVD processes; electron cyclotron resonance	Nitrides, carbides, and borides
Thermal decomposition	Gaseous and condensed precursors	Nitrides and borides
Nitridation and hydridation	Low-temperature version; implantation	Nitrides and hydrides

tively rarely. Electron-beam evaporation (EBE) has been used to obtain carbide, boride, and carbidoboride (TiC/TiB_2) films.[34] This method has been used with heating of the substrates to high temperatures (650–1600 °C); the rate of deposition was up to 6 μm min^{-1} and the thickness of the layers was 0.25–0.3 mm, but their hardness was relatively low (up to 20–30 GPa) owing to intense recrystallisation. Laser evaporation (LE) is also used.

The thermal vaporisation of metals and alloys in a reaction medium with simultaneous saturation by the interstitial elements (carbidation, nitridation and hydridation) is more common. A version of this method — activated reactive evaporation (ARE) — is particularly well known, although the latter is 'akin' to ion deposition processes. Laser reactive sputtering of niobium targets in carbon-containing media for the preparation of superconducting niobium carbide films has been described.[35] The use of a glow discharge and of other plasma-activating processes for these purposes is known,[36] but the most effective variety of the ARE is arc vapour ion deposition (sputtering) (AVID).

In order to obtain IP films by the thermal vaporisation method, account must be taken of the characteristic features of this process. The compounds from which films are obtained possess in most cases wide ranges of homogeneity and vaporise predominantly (at least in the initial stage) incongruently. The possibilities of statistical-thermodynamic methods, which make it possible to estimate the rates of vaporisation and the congruently vaporising IP compositions have been examined in monographs.[2, 19]

The vacuum vaporisation of intermetallic compounds of the type FeTi and $LaNi_5$ with subsequent hydridation (VViH) is also used to obtain hydride films (see, for example, Singh et al.[37] and Li and Cheng [38]).

b. Ion plating

The term 'ion plating' was first encountered in the communication of Mattox and McDonald [39] for the designation of a wide range of plasma-activated PVD processes in which the surface of the support was subjected to the action of an ion stream before the deposition of the film. The excitation of an arc discharge in a nitrogen or carbon-containing atmosphere is one of the most common variants of this technology, which has found extensive industrial application (on 'Bulat' type devices in our country). Metallic cathodes are used as a source of metal ions in AVID, high degrees of ionisation being attained under these conditions (from 30% to 100%), the kinetic energy of the ions is from 10 to 200 eV, and the rate of deposition may be up to 1–3 μm min^{-1}.[40, 41]

In most cases $Ar + N_2$ or $Ar + C_nH_m$ reactive working media at a pressure of $\sim 10^{-3}$ mm Hg and metallic cathodes (Ti, Ti–Al, Zr, Mo, Cr, etc.) are used in AVID. The principal deficiency of AVID is the formation of the so-called drop phase as a result of the intense influence exerted by the arc on the cathode and the high probability that metal drops enter into the films deposited. Filtered AVID processes, where the drop phase can be to a large extent filtered off by means of a magnetic field, are known.[24, 42, 43] Also known are hybrid variants of PVD, including both multicathode devices and a combination of AVID and magnetron sputtering (MS), which makes it possible to obtain a wide variety of types of multilayer and doped films.[44]

A more flexible variety of ion deposition is MS. In magnetron sputtering, it is possible to employ not only metal and alloy cathodes but also cathodes made of IP as well as nonmetallic compounds and to reduce the temperature of the support to 100–200 °C and sometimes even below that. These factors greatly expand the possibilities for the preparation of films in amorphous and nanocrystalline states and also of supersaturated solid solutions. There are numerous variants of MS: d.c. sputtering, high-frequency sputtering, application of a bias voltage to the substrate, the use of so called unbalanced magnetrons, etc.[24, 26, 41] However, the degree of ionisation, the kinetic energy of the ions, and the rate of deposition are in almost all cases lower than for AVID (< 10%, up to 10 eV, and < 0.1–0.2 μm min^{-1} respectively).

Different variants of the ion-beam treatment (IBT), in which atoms are dislodged from the target by the bombardment of its surface with ion beams, have also come to be widely used. The ion beams are also employed for the treatment of the films formed. Figs 1 and 2 present two schemes for the ion-stimulated deposition of nitride films. In the first case, the metal ions are generated by bombarding a metallic target with inert gas or nitrogen ions and in the second a stream of metal atoms is generated by means of an electron-beam treatment.[45, 46] Such methods make it possible, on the one hand, to synthesise superstoichiometric compounds [45] and, on the other, to vary the crystallisation conditions. For example, bombardment with heavy ions (320 keV Ar^{2+} or 320 keV Xe^{2+}) in the deposition of TiB_2 films leads to the appearance of crystallinity even when the process is carried out

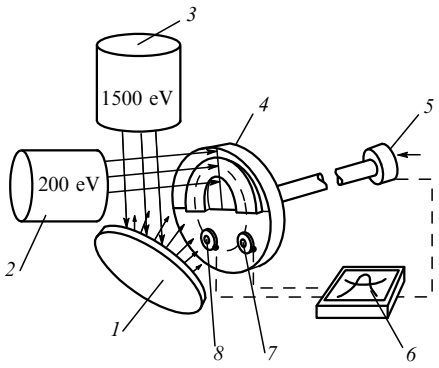


Figure 1. Schematic illustration of the binary ion-stimulated deposition of nitride films.[45]
(*1*) Target (Ti, Zr, Hf); (*2*) source of nitrogen ions or of a mixture of argon and nitrogen ions for the support; (*3*) source of argon, xenon, neon, or nitrogen ions for the target; (*4*) substrate; (*5*) angular mechanism rotation; (*6*) coordinate fixer; (*7*) current density counter; (*8*) rate of deposition counter.

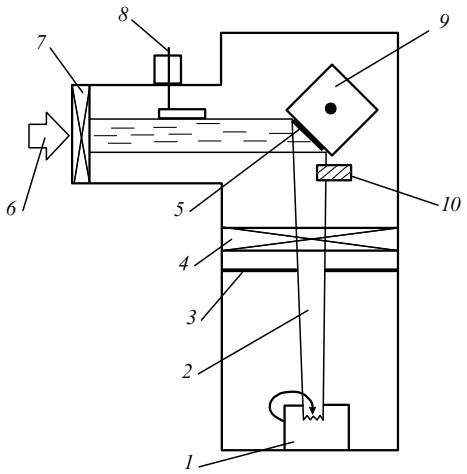


Figure 2. Schematic illustration of the EATON Z-200 IBED apparatus.[46]
(*1*) electron-beam vaporiser; (*2*) stream of vaporised metal atoms; (*3*) vaporisation lens; (*4*) separator; (*5*) substrate; (*6*) ion beam (N^+ or Ar^+); (*7*) separator; (*8*) ion beam current density counter; (*9*) cooled support holder; (*10*) rate of deposition counter.

at room temperature.[47] Only the formation of amorphous films was observed under these conditions without an ion-beam treatment. The use of molecular dynamics methods for IBT processes has been described.[48]

2. Chemical methods

a. Deposition from the gas phase

The traditional CVD technology, associated with high-temperature gas reactions of the type

$$TiCl_4 + \tfrac{1}{2}N_2 + 2H_2 \rightarrow TiN(s) + 4HCl, \quad (1)$$

$$TiCl_4 + \tfrac{1}{n}C_nH_m + H_2 \rightarrow TiC(s) + 4HCl + \left(\frac{m}{2n} - 1\right)H_2, \quad (2)$$

$$TiCl_4 + 2BCl_3 + 5H_2 \rightarrow TiB_2(s) + 10HCl, \quad (3)$$

has long been used to obtain wear-resistant protective layers, films, and general purpose coatings. Reactions (1)–(3) have been formulated in their final form but in fact they consist of many stages and in addition admixtures of oxygen complicate their occurrence in almost all cases. A comprehensive review of the studies devoted to wear-resistant TiN CVD coatings has been published.[27] Not only single-layer IP films but also multilayer and doped compositions of the type $Ti(C_xN_y)$, TiC + TiN, TiC + Al_2O_3, TiC + TiB_2, and TiC + Al_2O_3 + TiN have been developed and are manufactured on the industrial scale.[24, 27]

In most cases the temperature range for the deposition of CVD films is 900–1100 °C. Rates of deposition of 0.03–0.2 μm min^{-1} are typical for these conditions. The search for the possibility of reducing the process temperature, dictated mainly by the requirements of electronics and machine building, have led to the creation of different variants of physically stimulated regimes, in which plasma and laser techniques, electron cyclotron resonance (ECR), etc. are used.[49–54] The following features are characteristic of these variants:

(1) the deposition temperature is reduced to 600–300 °C and below;

(2) the rates of deposition are 0.001–0.2 μm min^{-1};

(3) organometallic precursors of the type of titanium tetrakis[dimethyl (or diethyl) amides] or tetraisopropoxide — $Ti[N(CH_3)_2]_4$, $Ti[N(C_2H_5]_4$ and $Ti[OCH(CH_3)_2]_4$ — having a high vapour pressure are used;

(4) compared with the usual CVD technology, these methods require special apparatus, so that their application is in most cases justified economically only in electronics.

Figure 3 presents a schematic illustration of the apparatus in which titanium tetrakis(dimethylamide) vapour and nitrogen are used and which is activated in an ECR cell.[51] The initial vacuum in the apparatus is maintained with the aid of a turbomolecular pump at a level below 10^{-10} mm Hg, while the working nitrogen pressure is 10^{-4} mm Hg. The temperature of the substrate, on which a shift potential is established, amounts to ~100 °C. The highest rates of deposition (~6×10^{-4} μm min^{-1}) and comparatively low electrical resistances of the films have been observed when a shift potential of −50 V was applied to the support. The composition of the films, monitored with the aid of XPES, proved to be as follows (at. %): Ti ~ 42, N ~ 42, C ~ 10, O ~ 6. Other schemes for the employment of ECR in order to obtain TiN films have been described. When these schemes are employed, the impurity content can be reduced by an increase in temperature but the rates of deposition remain nevertheless relatively low (~10^{-3} μm min^{-1}).[52–54]

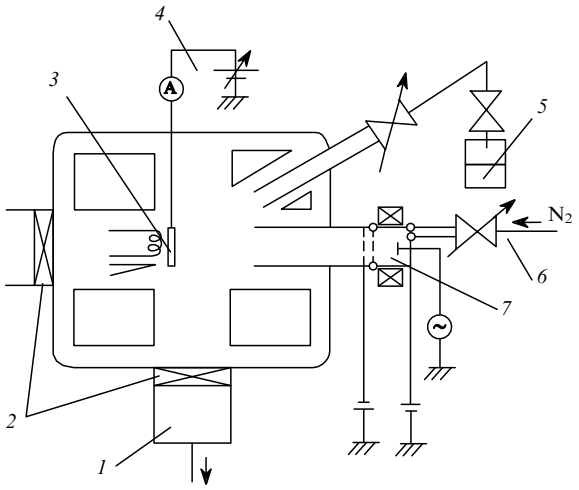


Figure 3. Schematic illustration of the apparatus for the deposition of TiN films using an organometallic precursor and the activation of nitrogen by means of cyclotron resonance.[51]
(*1*) turbomolecular pump; (*2*) nitrogen traps; (*3*) substrate with a device for heating and the measurement of temperature; (*4*) bias voltage source; (*5*) organometallic precursor (T = 75 °C); (*6*) supply of nitrogen; (*7*) cell of 90 W cyclotron resonance apparatus with a high-frequency generator and source and mains potential generators.

Examples of the synthesis of films comprising complexes of group IV and V transition metal tetrakis (dialkylamides) and ammonia at atmospheric pressure have been described.[55, 56] Fairly high rates of deposition (0.02–0.2 μm min^{-1}) and low temperatures (200–400 °C) were then noted and the impurity content was low; the formation of TiN, Zr_3N_4, Hf_3N_4, VN, Nb_3N_4, and Ta_3N_5 was detected. Epitaxial layer-by-layer growth of TiN film at 500 °C was observed when $TiCl_4$, and NH_3 were supplied alternately to the support with injection of zinc vapour after the supply of titanium chloride.[57]

It is seen from the foregoing that, in the course of the updating of the regimes in the traditional CVD technology, experimental data have accumulated and new schemes have been tested, but it is so far difficult to give preference to any one of them.

b. Thermal decomposition

The thermolysis of gaseous and condensed precursors for the preparation of IP films is used comparatively rarely. As regards titanium nitride and carbonitride films there have been indications that thermal decomposition of organometallic compounds of the type of titanium tetrakis(dialkylamides), including polymeric ones, is possible without the addition of ammonia to the reaction zone.[49, 58]

The deposition of titanium, zirconium, and hafnium boride films by the thermolysis of borohydrides has been described in several communications (see, for example, Refs 59–62). At fairly low decomposition temperatures (100–250 °C), the formation of both amorphous and crystalline films with a fairly high metallic conductivity is observed. The latter property is particularly attractive for the employment of these films in electronics as diffusion barriers. However, owing to the high reactivity of borohydrides, so far boride films are obtained by this method mainly on a laboratory scale.

c. Nitridation and hydridation

The nitridation and hydridation methods are applied in different variants: ionic and laser implantation of nitrogen and other interstitial elements in thin metallic films (Figs 1 and 2) or surface layers,[63–65] nitridation of surface layers in a high-frequency discharge,[66] high-temperature (400 °C) nitridation by hydrazine,[67] and hydridation of films at low temperatures including electrochemical and magnetron synthesis.[37, 38, 60, 69] However, compared with methods for deposition from the gas phase and thermal decomposition, nitridation and hydridation have no special advantages. Hydride films may be an exception, but the characteristic features of their preparation have so far been investigated on a limited scale.

III. Composition, structure, defects, and eletronic structure

The thickness of the films determines the application of the corresponding methods for their investigation.[70] This applies particularly to the study of their decomposition and defectiveness, for which many methods are employed; XPES, XRD, Auger electron spectroscopy (AES), scanning and transmission electron microscopy (SEM, TEM), Rutherford back scattering spectroscopy (RBSS), electron microprobe analysis (EMA), positron annihilation spectroscopy (PAS), secondary ion mass spectrometry (SIMS), scanning tunnelling and atomic force microscopy (STM, AFM), selected area electron diffraction (SAED), and others. In most cases, two and more methods are used to ensure the reliability of the results.

1. Composition

Table 2 presents certain results of the analysis of the composition of IP films obtained by different methods. The formulae of the films, found in a number of investigations,[51, 52, 54, 60, 72, 75, 76] were calculated by ourselves on the hypothesis that the boron, nitrogen, oxygen, and carbon atoms are located in one sublattice (for example, in octahedral positions), while the smaller hydrogen atoms are in another sublattice (for example, in tetrahedral positions). In many cases, the synthesis of IP films is accompanied by the formation of superstoichiometric compounds. The influence of argon pressure on the boron content in diboride (TiB_2 and ZrB_2), hexaboride [(La, Ce, Sm, Y)B_6], and dodecaboride (ZrB_{12}) films obtained with the aid of MS has been examined.[77] The formation of superstoichiometric phases in the first two cases and of prestoichiometric phases in the last case was noted. This was attributed to the characteristic features of the mobility and the collision reactions of the boron and metal atoms. The formation of superstoichiometric titanium carbonitrides and boridonitrides with the aid of MS has also been reported.[78] The important question concerning the relation between the compositions of the target and the sputtered film as regards IP has not so far been considered in detail. It has been noted[78] that the depletion in carbon of a nonstoichiometric titanium carbide ($TiC_{0.5}$) target has been detected with the aid of MS.

In the synthesis of the usual IP, the formation of superstoichiometric phases is observed mainly in the presence of oxygen impurities, which leads to the appearance of structural (nonthermal) vacancies in the metallic sublattice.[2, 7] The insufficiently complete attestation of the compounds listed in Table 2 precludes conclusions concerning the nature of the superstoichiometry of the IP films. Accurate measurements of the X-ray and pyknometric densities as well as detailed elemental and phase analyses are therefore needed. One should bear in mind that the agreement between the results of the determination of the elemental compositions of the films by various methods is not always satisfactory and this problem requires special consideration in almost every case.

Table 2. Compositions of certain IP films synthesised by various methods.

Compound	Method of preparation	Method of analysis	Ref.
$NbC_{0.75-0.98}$	LRS	XPES	35
$Ti(N_{0.72}C_{0.17}O_{0.11})_{1.38}$	ECR	"	51
$TiN_{0.74-1.07}H_{0.1-0.42}$	"	RBSS	52
$Ti(N_{\sim 0.9}C_{0.05}O_{0.03})_{0.8-1.3}H_{0.1-0.3}$	"	SIMS	54
TiN, Zr_3N_4, Hf_3N_4, $VN_{1.05-1.15}$, $NbN_{1.35}$, $TaN_{1.7}$	Low-temperature CVD	RBSS, XPES, SAED	55, 56
$Zr(B_{0.67}C_{0.17}O_{0.16})_{2.25}$	TD	AES	60
$TiN_{1.2}$, $ZrN_{1.5}$, $NbN_{0.9}$, $TaN_{0.8}$	Implantation	RBSS, XRD	64
$TiN_{0.8-1.2}$	DCMRS	RBSS, XPES, SAED, XRD	71
$(Ti,Al,Zr)(N_{0.96}O_{0.04})_{0.96}$	"	"	72
$TiN_{0.2-1.14}$	"	AES	73
$TiB_{2.1-2.85}$	HFMNS	AES, XRD	74
$Zr(N_{0.83}C_{0.13}O_{0.04})_{\sim 2}$	HFMRS	"	75
$Ti(B_{0.8}O_{0.11}N_{0.045}C_{0.045})_{2.5}$	HFMNS	AES	76

Note. The following designations have been adopted: LRS — laser reactive synthesis; ECR — electron cyclotron resonance; TD — thermal decomposition; DCMRS and DCMNS — direct current magnetron reactive and nonreactive (i.e. sputtering by neutral atoms) sputtering respectively; HFMRS and HFMNS — high-frequency magnetron reactive and nonreactive sputtering respectively.

Oxygen is one of the commonest impurities in IP. Fig. 4 presents the dependence of the titanium, nitrogen, oxygen, and carbon concentrations on the surfaces of TiN films on the partial pressure of oxygen in a direct current magnetron reactive sputtering (DCMRS) chamber. The plots were constructed from results obtained by the AES method *in situ*.[79] Analysis demonstrated how important is the 'vacuum hygiene' in the preparation of IP films: at an oxygen partial pressure in excess of $\sim 10^{-6}$ mm Hg (total pressure $\sim 10^{-3}$ mm Hg), a decrease in the nitrogen concentration and an increase in the oxygen impurity content are observed. A similar situation has been noted also for water vapour.

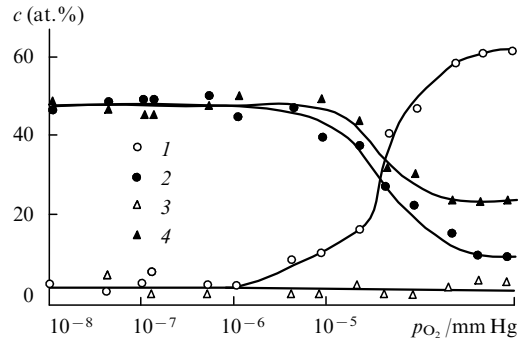


Figure 4. Dependence of the concentrations of oxygen (*1*), nitrogen (*2*), carbon (*3*), and titanium (*4*) on the surfaces of TiN films on the partial pressure of oxygen.[79]

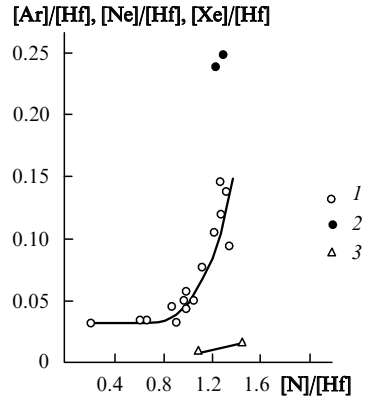


Figure 5. Variation of the contents of argon (*1*), neon (*2*), and xenon (*3*) in the region of homogeneity of hafnium nitride.[45]

The presence in the films of inert gas atoms, entrained in the course of sputtering and implantation, is noteworthy. Fig. 5 presents the dependence of the argon, neon, and xenon contents on the composition of hafnium nitride films synthesised in accordance with the binary ion-stimulated deposition scheme (Fig. 1). The content of the inert gases increases significantly with increase in the amount of nitrogen in the superstoichiometric nitrides, the total amount of these gases being, as expected, inversely proportional to their atomic radius. The above concentration dependence may be associated with increase in the concentration of structural vacancies in the nonstoichiometric phases. An approximately similar situation has been observed also for titanium and zirconium nitrides.

Interesting possibilities of XPES in relation to the analysis of $Ti(B,N)_x$ films have been demonstrated by Mollart et al.[80] Fig. 6 presents the XPE spectra of the 1*s* states of boron and nitrogen in

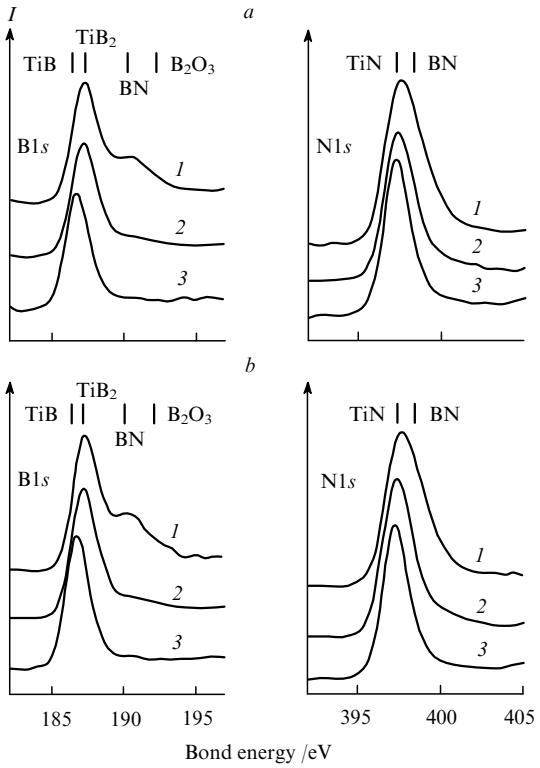


Figure 6. XPE spectra of the 1*s* states of boron and nitrogen in nitridoboride films of different composition before annealing (*a*) and after annealing at 400 °C (280 min) (*b*).[80]
(*1*) TiB_2N; (*2*) $TiBN_{0.5}$; (*3*) $Ti_2BN_{0.5}$.

nitridoboride films of different composition in the initial and annealed states. The films were obtained by the direct current magnetron nonreactive sputtering (DCMNS) method using Ti – BN composite targets of different composition. By employing standards for TiB, TiB_2, BN, and B_2O_3, it was possible to estimate with an accuracy of ±30% the phase compositions of different films, which agreed qualitatively with data obtained from the Ti – B – N phase diagram. The XRD and AES methods proved less informative in this respect, although the latter has been recommended for the determination of the [N]/[Ti] ratio in titanium nitride.[81]

2. Structure and defects

a. Lattice parameters and occupancy of sublattices

The IP structure began to be investigated a long time ago, but an insufficiency of results obtained on well attested objects is nevertheless still felt. It was noted above that accurate measurements of the X-ray and pyknometric densities are needed for the elucidation of the occupancy of the metallic and nonmetallic sublattices in IP. Such densities are nontrivial for low dimensionality objects such as films.

A decrease in the lattice parameter on deviation from stoichiometry has been noted for both the usual[82] and film[22,83] titanium nitride specimens (Fig. 7). A similar situation is characteristic also of hafnium nitride.[84] The absolute values of the lattice parameters for IP films are usually greater than for massive specimens. This is as a rule attributed to the influence of the residual stresses, the grain size, and also the presence of impurities. It is striking that the period depends on the film thickness. A decrease in the lattice parameter with increase in the thickness of TiN, NbN, and CrN films has been noted (it is particularly marked up to a thickness 50 – 150 nm); on the other hand, for a zirconium nitride film the lattice parameter also increases with increase in thickness.[85] The presence of an appreciable crystallographic anisotropy in the lattice deformation parameters for the substoichiometric and stoichiometric titanium nitrides is also of interest.[83] Thus the relations $a(200) > a(111)$ and $a(200) < a(111)$ are characteristic of $TiN_{\sim 0.55}$ and $TiN_{\sim 1.0}$ respectively. The latter relation is also observed for superstoichiometric TiN films, which has been attributed to the possible formation of a phase with a CaF_2 type structure in the form of nanocrystals.[86] However, an unambiguous treatment of these and other changes in the lattice period in IP films requires additional studies and a detailed elemental analysis.

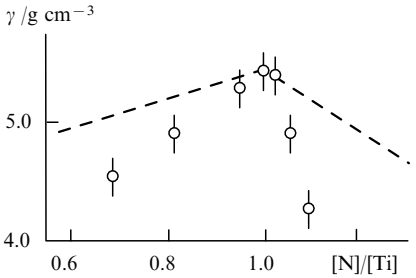


Figure 7. Variation of the density (γ) in the region of homogeneity of titanium nitride films.[32]
Dashed line — calculated results obtained. on the basis of a purely vacancy approach.

In a number of investigations, the point defects in the films were studied by positron annihilation spectroscopy.[84, 87 – 89] The presence of defects of the type of vacancies, interstitial atoms, micropores, and others has been noted. However, the treatment of the annihilation characteristics in IP with different sublattice occupancy is still far from being fully understood, so that neutron diffraction studies with determination of the locations of light

atoms and of the ordering of structural vacancies might therefore 'throw light' on this problem.

Certain interesting features of the crystal structures of Ti(Si, N, O), NbN, ZrN, LaB_6, CeB_6, SmB_6, ZrB_2, and TiB_2 films (anisotropy of the lattice parameters, the influence of the film thickness on the crystallinity), as well as single crystal film deposition processes, the formation of supersaturated solid solutions, etc. have been examined in a number of investigations.[77, 90–94] The characteristics of the ordering in IP films remain virtually little investigated, although an appreciable amount of information has accumulated for these compounds in the usual (nonfilm) form.[2, 10, 20]

b. Residual stresses and texture

The residual stresses in IP and their structure have been thoroughly investigated and described in the literature (see, for example, Refs 22, 24–26, 83, and 95–97). The residual macrostresses are measured by an X-ray method (the so called $\sin^2\psi$ method) and many mechanical methods. It is believed that the residual stresses are due to the difference between the coefficients of linear thermal expansion of the film and the substrate and also to the characteristic features of the film growth. For the majority of PVD films, these stresses are compressive; for TiN CVD films, tensile stresses have been noted.[25] Appreciable compressive stresses have been detected also for TiC and TiB_2 PVD films.[22, 93] It has been observed that the bias voltage and ion bombardment exert a significant influence on the residual stresses.[26, 83] In the region of homogeneity of TiN, the residual stresses vary nonmonotonically, minimum stresses being characteristic of the $TiN_{\sim 0.7}$ composition, to which the maximum hardness corresponds (see below).[95]

The study of the texture of TiN CVD films revealed that the preferred orientations depend on the deposition temperature and on the molar ratio $[TiCl_4]/[NH_3](m_{[N]/[Ti]})$.[98] Three types of preferred orientations have been detected; the <100> texture is characteristic of low deposition temperatures; the <110> texture corresponds to moderate temperatures and low values of $m_{[N]/[Ti]}$; the <111> texture corresponds to high process temperatures and high values of $m_{[N]/[Ti]}$. The changes in the nature of the texture are attributed to the characteristic features of the supersaturation in the gas phase. Weber et al.,[52] who used the ECR method to activate nitrogen, noted that the preferred <200> orientation was observed for TiN films when N_2 was employed, while the <111> texture was characteristic of the film when ammonia was employed. It has also been noted that the latter texture is manifested for titanium nitride (PVD) with a nearly stoichiometric composition ($TiN_{0.88-1.0}$); for compositions with a lower nitrogen content, the <311> and <200> textures predominate.[95] The influence of substrate layers (titanium nitride or carbide) on the textures of AVID carbide and nitride films respectively and also of multilayer nitride films has been analysed.[85, 97]

The influence of film thickness and partial nitrogen pressure in PVD processes has been investigated.[99, 100] With increase in film thickness from 1.3 to 6.8 μm, the preferred texture changed from the <200> orientation to <111>; the opposite change was observed when the partial nitrogen pressure was increased, which was accompanied by a decrease in the residual compressive stresses. Such changes in texture are associated with the deformations accumulating during the deposition of the films when account is taken of the anisotropy of the surface energies of different crystallographic faces.

Figure 8 illustrates the influence of the thickness of the TiB_2 films obtained by the DCMRS method on the nature of the X-ray peaks.[93] The ratio of the intensities of the (001) and (101) reflections is manifested fairly clearly only for thicknesses in excess of 1300 Å. A predominantly random orientation is characteristic of thinner films (Fig. 8*a*), while the <001> texture begins to be manifested distinctly when the thickness increases.

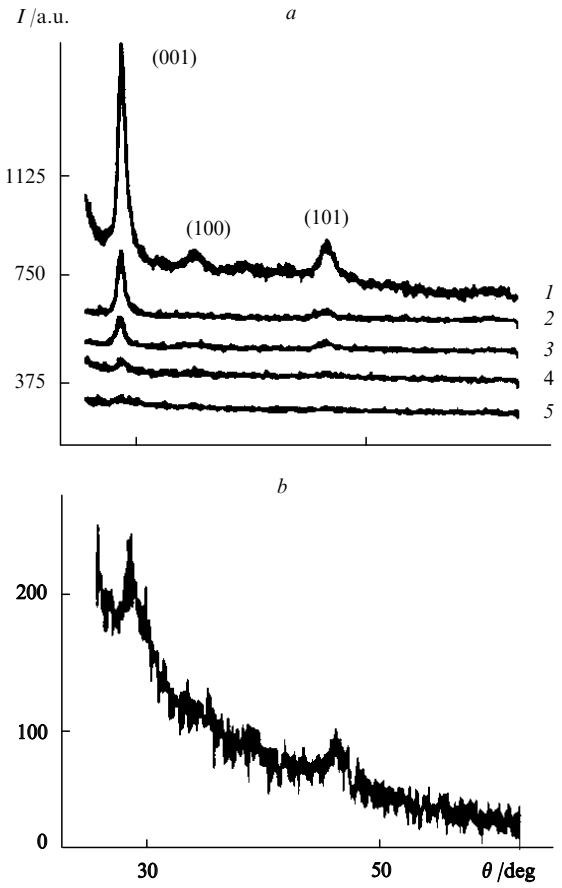


Figure 8. Diffractograms for a TiB_2 film obtained at an angle of 5 °.[93] (*a*) the influence of thickness; (*b*) film 860 Å thick; film thickness (Å): (*1*) 5000; (*2*) 2800; (*3*) 1800; (*4* 1300; (*5*) 860.

The thermal stability of texture orientations in IP films has been investigated on a limited scale.

c. Grain size (of crystallites) and morphology

The study of the fine structure [the size of the crystallites (L) and microstrains (ε)] and also of the morphology of IP films is needed to elucidate their properties. Fig. 9 presents the (200) and (111) reflections for a titanium nitride film obtained in accordance with the ion-stimulated deposition scheme (Fig. 2).[46] The broadening of the peaks as the energy of the Xe ions is varied can be seen. The quantity L is estimated from the familiar Scherrer formula using the measured peak width at half-height level. For accurate calculations, it is necessary to take into account the contribution of microdistortions to the width of the peaks. For this purpose, use is made of different modifications of the familiar Warren–Auerbach and Williamson–Hall methods.[101]

Table 3 presents certain results of the determination of the values of L and ε for IP films. The size of the crystallites in the films investigated is in most cases < 50 nm and they can therefore be assigned to the class of nanocrystalline (nanostructural) objects. A detailed study of the influence of the temperature of the substrate, the bias voltage, and the duration of sputtering on the value of L estimated from the width of the (111) reflection has been undertaken for TiN.[105] It is of interest that the influence of temperature is manifested distinctly only for a bias voltage of about −60 V,whereas at −100 and −200 V it is virtually absent in the temperature range 150–500 °C. The influence of various factors on L and ε for the magnetron sputtering of a wide variety of targets (TiNi, $TiC_{0.5}$, TiB + Ti, etc.) has been described.[78, 107] It was noted in the same investigations, in particular, that the reason for the difference between the values of L determined by the XRD

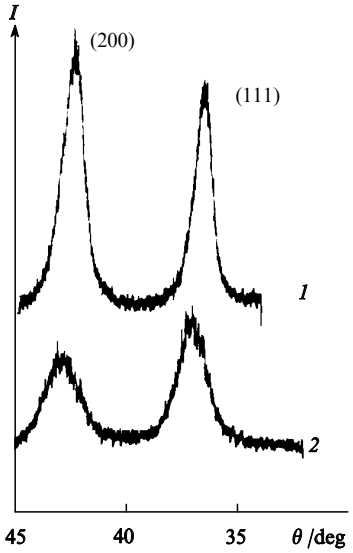


Figure 9. Overall form of the (200) and (111) reflections for a TiN film.[46] Energy of xenon ions (kV): (*1*) 40; (*2*) 20.

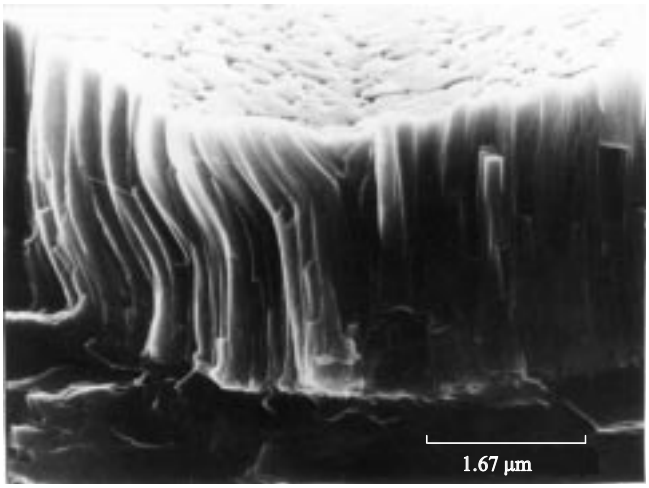


Figure 10. The fracture surface in a TiN film in the region of indentation by the microhardness measuring device.
The photograph was taken on a high-resolution scanning electron microscope (FEG-SEM) and has been kindly provided by Ma and Bloyce.[110]

Table 3. Dimensions of crystallites and the magnitude of microdistortions.

Compound	Method of preparation	L / nm [a]	$10^3\,\varepsilon$	Ref.
$TiN_{0.48-1.0}$	AVID	9–21	0.8–2.6	95
TiN	IBT	4–8	–	102
Ti_2N	"	6–21	–	102
TiN	"	5–20	–	46
TiN	AVID	20	–	103
	DCMRS	35	–	103
TiN	"	23–66	0.8–13	104
TiN	"	30–140	–	105
ZrN	HFMRS	–	9	91
NbC	DCMNS	30–140	–	106

[a] The values of L were estimated from the Scherrer formula in addition to the results obtained from the literature.[91, 95, 104]

and TEM methods may be packing defects, which contribute to the broadening of the X-ray reflections and the block nature of the structure. Such differences for nanocrystalline materials are fairly frequent,[101] which is associated with the columnar nature of the morphology of many IP films. A combination of various methods for the determination of L is therefore needed, particularly in relation to multilayer objects.[96]

The presence of edge misfit dislocations with a Burgers vector 1/2 [110], characteristic of carbides and nitrides with the NaCl structure, has been detected in multilayer TiN, NbN, VN, and (TiV)N films, which were deposited by the DCMRS method on the (100) face of a MgO single crystal.[108] The relaxation of the stresses with formation of a domain structure under the influence of the differences between the lattice periods and layer thicknesses has been observed. The density of the loop dislocations fell from 5×10^{12} to 1.5×10^{10} cm^{-2} with increase in the temperature of the single crystal support from 550 to 850 °C, which ensured the formation of single crystal TiN films.[109]

The morphology of the structural features of IP films may be characterised as columnar and as random with a wide range of intermediate variants. Fig. l0 presents a typical columnar structure of a TiN film obtained by the DCMRS method.[110] In cross section, the size of the crystals reaches 200–300 nm. This photograph clearly illustrates also the presence of a residual plastic deformation of the fibres of the brittle titanium nitride in the region of the microindentation. The influence of the deposition temperature and of the shift potential on the morphology of TiN films has been described.[105] Depending on the deposition conditions, in cross section the form of the crystals varied from triangular to square and their size was between 50 and 500 nm, which is greater by factors of 2–4 respectively than the X-ray determinations of L (Table3). This difference must be attributed to the approximate nature of the estimates from the Scherrer formula. Another type of fracture in TiN films obtained by the DCMRS method in apparatus with four planar nonbalanced magnetrons (a columnar amorphous structure) has been described by Effoglu et al.[111] The possibility of obtaining columnar structures by employing stronger magnetic fields was demonstrated in the same study. It is of interest that films with a noncolumnar amorphous structure had more effective mechanical and operational properties. It has also been noted that the imposition of a shift potential during magnetron sputtering promotes the elimination of the porosity of the films.[112]

The study of the fractures in boride films (see, for example, Refs 74, 76, 77, 113, and 114) revealed different structural types. A stone-like fracture or a 'cauliflower' type fracture with a partially manifested columnar structure is characteristic of these films, the columnar structure becoming more pronounced with increase in the nitrogen content (Figs 11 and 12). The porosity of the films is usually low or virtually absent, but it must nevertheless be taken into account in the analysis of the properties of the films. The

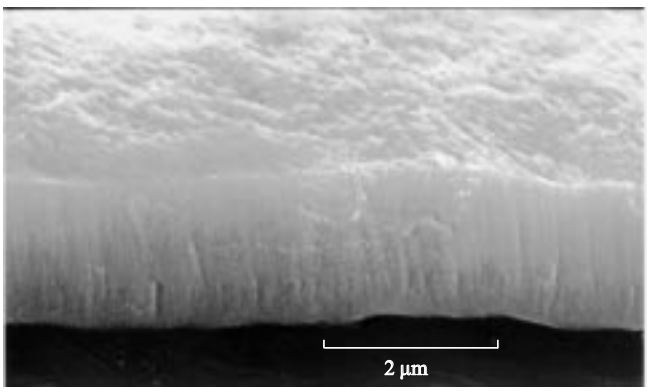


Figure 11. The fracture surface in a TiB_2 film obtained by the DCMNS method.[114]

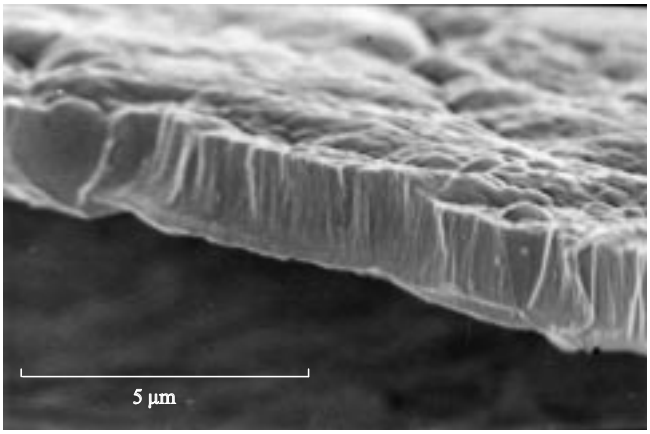


Figure 12. The fracture surface in a $Ti(B,N)_x$ film obtained by the DCMNS method.[114]

methods for the determination of porosity from electrochemical measurements in relation to TiN, Ti(B, N), and (Ti, Al)N films have been described by Aromaa et al.[115] and the general features of the macro- and micro-defects in the coatings have been analysed in a monograph.[116] We may note that the general level of the porosities of films obtained by the IBT and HFMNS methods was from 0.003% to 0.239%.[115] The topography of the film surfaces was investigated both with the aid of scanning electron microscopy (Figs 10–12) and (especially) scanning tunnelling and atomic force microscopy.[117]

The characteristic features of the morphology of the IP films obtained with the aid of CVD technology have been examined in a series of studies (see, for example, Refs 27, 55, and 118–120). It is important to note that, when two- or three-phase systems (compositions such as TiB_2–TiC, SiC–TiC–C, TiN–AlN, etc.) are codeposited, nanostructural multilayer and mixed films, coatings, and layers with $L \approx 10$–20 nm may be obtained judging from the equilibrium phase diagrams. By virtue of the high process temperatures ($\sim$1000–1100 °C), the rates of deposition are very high ($\sim$1 mm h^{-1}). For the SiC–TiC–C nanocomposites, a texture in the growth of (Si, Ti)C crystallites with a transverse dimension of 10–15 nm in the <220> direction was noted; according to Raman spectroscopic data, the size of the graphite inclusions did not exceed several nanometers.[119]

Thus a wide spectrum of morphological structures, caused by the diverse influence of the deposition conditions, impurities, and other factors in the PVD and PCD processes, is characteristic of IP films. In a number of studies (see, for example, Refs 24, 26, 121, and 122), attempts were made to put forward schemes which would make it possible to predict the formation of particular structures in the PVD films. The prediction was based on the analysis of homologous deposition temperatures, the gas pressure, the shift potential, etc. Estimates of the conditions for the production of single crystal and polycrystalline formations are available for CVD films.[123] However, in the vast majority of cases the predictions are so far qualitative in character.

A schematic illustration of typical morphological structures is presented in Fig. 13 in relation to TiN and $(Ti_{0.5}Al_{0.5})N$ PVD films. The authors of this scheme[28] note that, apart from the principal factors indicated (deposition temperatures and ionic characteristics), parameters such as the composition of the plasma-forming gas, the impurities, etc. may greatly alter the nature of the morphology of the deposited films. The wide variety of factors exerting an influence, listed above, does not as yet permit an *a priori* prediction of the formation of particular morphological structures and this question requires further study.

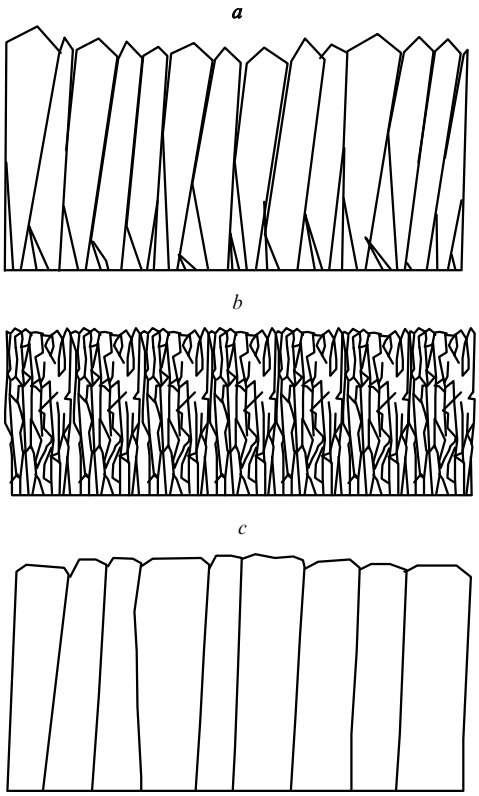


Figure 13. Schematic illustration of typical morphological structures of TiN and $(Ti_{0.5}Al_{0.5})N$ PVD films.[28]
(*a*) low deposition temperatures ($T < 500$ °C) and low energy characteristics of the ions; (*b*) low deposition temperatures and average energy parameters of the ions (100–500 eV) (*c*) high deposition temperatures ($T > 500$ °C) or low temperatures but high low-energy ion fluxes.

3. Electronic structure and chemical bonding

The electronic structure and chemical bonding in carbide and nitride films have been investigated by numerous workers (see, for example, Refs 21, 55, 56, 84, and 125–128). One of the latest communications devoted to this problem is a review.[124] The binding energies of Ti $2p_{3/2}$, B 1*s*, and N 1*s* core levels have been measured[80, 125, 127] for $Ti(B,N)_x$, TiB_2, and TiN films as well as those of the Ti 2*p*, N 1*s*, and O 1*s* levels for TiN_x and $Ti(N,O)_x$ films. The effective charges on the titanium, oxygen, and nitrogen atoms have been estimated.[127] The possible influence of structural deflects in IP on the binding energies of the core levels and the difficulties in understanding the nature of the IP have been discussed.[84] Detailed XPES studies on cubic (Ti,Al)N films as well as quantum-chemical calculations made it possible to estimate the effective atomic charges and the distribution of the local density of states and to conclude that there is an ionic component in the bonds.[124, 126] Comparison of the estimated cohesion and substitution energies in titanoaluminium nitrides and carbides showed that the formation of the latter is less probable.

Table 4 presents the experimental binding energies for the 1*s* levels of nitrogen and the levels of the metals in Group IV and V transition metal nitride films synthesised from organometallic precursors and ammonia at low temperatures.[55, 56] These films were characterised by a low content of impurities (less than 1–2 at. % of oxygen and carbon) and by the small size of the crystallites ($L \approx 2$–5 nm). However, the hydrogen content, characterised by the ratio [H]/[M], varied in the range 0.5–1.35. The

Table 4. The binding energies (eV), found by the XPES method, for films deposited at 200 °C.[55, 56]

Compound	Precursor	Energy of N 1*s* level	Energy level of metal atom	E_M
TiN	$Ti(NMe_2)_4/NH_3$	396.9	Ti $2p_{3/2}$	454.8
Zr_3N_4	$Zr(NMe_2)_4/NH_3$	397.2	Zr $3d_{5/2}$	180.3
Hf_3N_4	$Hf(NMe_2)_4/NH_3$	397.0	Hf $4f_{7/2}$	15.1
VN	$V(NMe_2)_4/NH_3$	397.0	V $2p_{3/2}$	513.1
Nb_3N_4	$Nb(NEt_2)_4/NH_3$	397.4	Nb $3d_{5/2}$	204.1
Nb_3N_4	$Nb(NMe_2)_5/NH_3$	397.2	Nb $3d_{5/2}$	203.9
Ta_3N_5	$Ta(NMe_2)_5/NH_3$	396.9	Ta $4f_{7/2}$	24.0

binding energies in the films do not differ from those for the nitrides in the usual polycrystalline state [55, 56] and it has not so far been possible to detect a possible change in the electronic structure in the nanocrystalline state.

IV. Properties

1. Electrical and optical characteristics

a. Electrical resistivity

The metal-like nature of the interstitial phases is manifested primarily in their electrical properties — a low specific resistance (ρ) and a positive coefficient of its temperature dependence ($\alpha = \Delta\rho/\rho\Delta T$). This is associated with the characteristic features of the energy spectrum of the electrons in IP and with the high concentration of carriers.[2, 7, 17] The level of the resistivity in some of the IP (for example, stoichiometric Group IV transition metal nitrides and borides) is appreciably lower than in the corresponding metals. On the other hand, certain superstoichiometric IP, in particular nitrides, behave as semiconductors and dielectrics. The deviation from stoichiometry has a great influence on the electrical properties. Furthermore, as in the case of metals and alloys, ρ and α are greatly influenced by the overall impurity content and the defectiveness of the structure, including the grain size and the cross-section of the specimens (we have in mind the scattering of the carriers at the grain boundaries and on the outer surfaces). The study of electrical properties is a fairly representative method for the investigation of the composition and ideality of IP films, but a detailed attestation of the test objects is then of course required.

Table 5 presents the results of the determinations of ρ for IP films obtained by different methods. Not all the data are presented, but only those which are most reliable (in this sense the results for TiN are outstanding). In a number of instances, one should not overestimate the value of the information presented, since there are no detailed data on the composition, defectiveness, and thickness of the films. Nevertheless, we shall emphasise certain general characteristics of the results presented in Table 5.

1. The variation of ρ in the region of homogeneity of the IP is not monotonic. This is illustrated in Fig. 14 for TiN, ZrN, and HfN films synthesised in accordance with the ion-stimulated deposition scheme (Fig. 1).[45] The increase in ρ on deviation from stoichiometry in the decreasing direction ($n < 1$) is usually attributed to the scattering of the carriers by structural vacancies in the nonmetallic sublattice. The considerable increase in ρ for $n > 1$ is due to the transition to compounds with nonmetallic conductivity. A similar situation has been observed for yttrium and lanthanum dihydride and trihydride films.[146] We may also note that, on the one hand, the variation of the electron energy spectra on passing from MN to M_3N_4 has been confirmed also by quantum-chemical calculations [149] and, on the other, the fact that the concentration of inert gases increases in the superstoichiometric nitrides (Fig. 5). At the same time a different type of variation of ρ may be observed in the region of homogeneity, for example, ρ for tungsten nitride films diminishes on deviation from stoichiometry.[136]

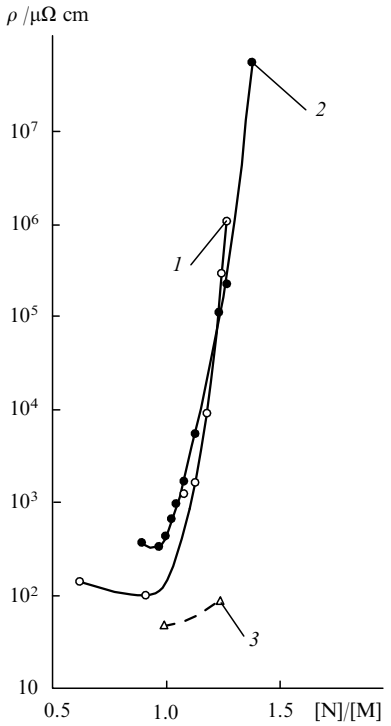


Figure 14. Variation of the resistivity in the region of homogeneity of HfN (*1*), ZrN (*2*), and TiN (*3*).[45]

2. By comparing the overall level of the values of ρ with the available data for IP (see, for example, Refs 2, 7, and 17), one may note that results indicating a high degree of ideality and a low impurity content have been obtained only in isolated instances (TiN single crystal films [129] and extremely ideal ZrN films [132]). This was achieved by employing single crystal supports (MgO and Si) and by the thorough maintenance of other deposition conditions (high temperatures, low ion energies, 'vacuum hygiene', etc.).

Figure 15 presents the dependences of ρ and of the width of the (200) reflection for a ZrN film on the of energy nitrogen ions.[132] The low values of ρ were determined by the deposition temperature (not above 800 °C) and the corresponding specified generation of nitrogen ions and zirconium atoms ensuring the formation of a zirconium nitride with a nearly stoichiometric composition. The influence on ρ by various conditions in the deposition of TiN films on single crystal silicon supports with a germanium sublayer under the conditions of pulsating laser vaporisation has been analysed in detail.[131]

3. It has been noted [57] that minimal values of ρ have been obtained for a thickness of a TiN CVD film greater than l00–150 nm. For PVD films, the critical thickness was

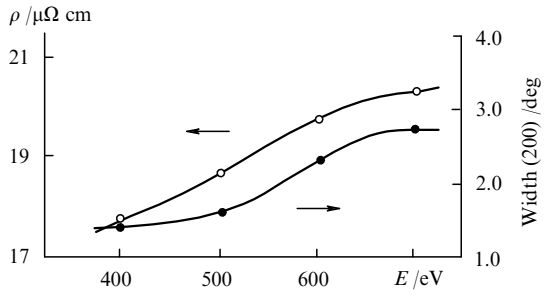


Figure 15. Dependence of the resistivity and the width of the (200) reflection for a ZrN film on the energy of nitrogen ions.[132]

Table 5. The resistivities (ρ) of IP films at room temperature.

Film	Method of preparation	ρ /μΩ cm	Ref.	Film	Method of preparation	ρ /μΩ cm	Ref.
Nitrides				Carbides			
$Ti_{\sim 2}N$	DCMRS	~200	22	$ZrC_{0.9}$	ARV	560	137
$Ti(N_{0.72}C_{0.17}O_{0.11})_{1.38}$	ECR	~250	51	$NbC_{0.98}$	LV	20–50	35
$Ti(N_{0.68}C_{0.22}O_{0.10})_{1.44}$	"	~600	51	$NbC_{\sim 1.0}$	"	4 (T = 4 K)	138
$TiN_{0.86}$	"	45	52	Borides			
$TiN_{1.02}H_{0.15}$	"	100	52	$TiB_{\sim 2}$	HFMNS	500 (150)	139
$TiN_{\sim 1.2}$	DCMRS	120	71	$TiB_{1-2.1}$	DCMNS	~260 (120)	140
$TiN_{1.06}$	ARV	82	73	$TiB_{\sim 2}$	"	~150	141
$TiN_{0.98}$	"	110	73	$ZrB_{\sim 2}$	"	250 (75)	139
$TiN_{\sim 1.0}$	DCRMS (single crystal film)	18	129	$TiB_{\sim 2}$	HFMNS	296	141
$TiN_{\sim 1.0}$	AVAD (filtered)	20	130	$ZrB_{\sim 2}$	"	250 (75)	139
$TiN_{\sim 1.0}$	LV	26	131	$Zr(B_{0.67}C_{0.17}O_{0.16})_{2.25}$	TD (T = 100–270 °C)	150	60
Zr_3N_4	CVD (T = 200–400 °C)	> 10^6	55	HfB_x	HFMNS	~370	142
$ZrN_{\sim 1.2}$	HFMRS	~100	75	$HfB_{\sim 2}$	"	~230	143
$ZrN_{\sim 1.0}$	IBT	17.8	132	$YB_{\sim 2}$	EBE	55	144
Hf_3N_4	CVD (T = 200–400 °C)	> 10^6	55	$YB_{\sim 4}$	"	51	144
HfN_x	HRMRS	~200	133	$YB_{\sim 6}$	"	88	144
VN_x	CVD (T = 200 °C)	~10^3	56	$LaB_{\sim 6}$	DSMNS	104	144
Nb_3N_4	CVD (T = 200 °C)	10^3–10^4	56	Hydrides			
$NbN_{\sim 1.0}$	ECR	75	92	$TaH_{0.48}$	EBE and hydridation	~46	145
$Ta_{\sim 2}N$	HFMRS	200	134	$YH_{\sim 2.0}$	VViH	~50	146
Ta_3N_5	CVD (T = 200 °C)	> 10^6	56	$YH_{\sim 2.85}$	"	~10^4	146
$MoN_{\sim 1.0}$	DCRMS	~480	135	$LaH_{\sim 2.0}$	"	~40	146
$W_{\sim 2}N$	"	~400	135	$LaH_{\sim 2.85}$	"	~10^5	146
Carbides				$LaNi_5H_x$	"	~670	147
$TiC_{\sim 1.0}$	ARV	40	137	$LaCo_5H_{\sim 0.5}$	"	350–660	148
$TiC_{0.8}$	CVD	196	137	$SmCo_5H_x$	"	360–440	148

30–40 nm,[150] although the most reliable results were obtained for a thickness of ~260 nm; a preliminary consideration of the role of the scattering of carriers at intergrain boundaries and on the film surfaces has been carried out. These questions appear to have been inadequately investigated for IP films.

4. The results presented for carbide, boride, and hydride films indicate that the optimum conditions for their preparation with an ideal structure have not so far been found. The values of ρ for annealed specimens are indicated in brackets for $TiB_{\sim 2}$ and $ZrB_{\sim 2}$ films, but one should recall that the resistivity ρ of boride single crystals may be an order of magnitude lower (see, for example, Zhurakovskii and Nemchenko [17] and Serebryakova et al.[18]).

An important parameter reflecting the influence of purity and ideality and also containing information about the nature of the carriers is the coefficient of the temperature dependence of the resistivity (α). Table 6 presents results reflecting the influence of the conditions in the deposition of TiN films by the HFMRS method on ρ and α and superconducting characteristics. These data clearly indicate the high structural sensitivity of the electrical characteristics. We may note, that according to the results of Johansson et al.,[129] $\alpha = 6.2 \times 10^{-3}$ K^{-1} for ideal single, crystal TiN films (ρ = 18 μΩ cm) (for a film ~260 nm thick, $\alpha = 6.4 \times 10^{-3}$ K^{-1})[150]. It has been reported in a review [22] that $\alpha = (1-2) \times 10^{-3}$ K^{-1} for the majority of the usual TiN films. A negative value of α is characteristic of the nonmetallic type of conductivity, for example, in the case of Zr_3N_4 films.[76] A different sign of α has been noted for NbN films: positive for single crystal films [92] and negative for polycrystalline films.[151]

Table 6. The influence of the conditions in the deposition of TiN on the resistivity (ρ), the temperature coefficient of the resistivity (α), the temperature of the transition to the superconducting state (T_c), and the width of the superconductivity transition (ΔT_c) (film thickness 30–100 nm).[150]

Temperature of support/ °C	Bias voltage /V	ρ /μΩ cm	$10^3\alpha$ /K^{-1}	T_c /K	ΔT_c/K
40	0	205–215	0.26	< 4.3	0.04
40	−115	120–135	0.56	< 4.3	0.04
500	0	65–70	1.02	4.84	< 0.02
500	−100	45–60	1.34	5.04	< 0.02

A detailed study of the electrical properties of epitaxial single crystal multilayer TiN–VN films has been undertaken.[152] Measurements of the Hall constant (R_H) and ρ showed that r_H (and hence the concentration of carriers $n = 4.5 \times 10^{22}$ cm^{-3}) is independent of the thickness of the layers, while ρ and the mobility of the carriers (m) increase sharply, like α, with decrease in thickness, starting with 6 nm. For layers more than 10–15 nm thick, the following values were obtained: $\rho \approx 30$ μΩ cm, $m \approx 5$ cm^2 V^{-1} s^{-1}, and $\alpha \approx 1.6 \times 10^{-1}$ K^{-1}. Estimation of the free path length (λ) of the electrons within the framework of Drude's model and on the assumption that the Fermi surface is spherical led to $\lambda \approx 4.6$ nm (both for TiN and VN). These estimates are approximate because, for example, the Fermi surface for nitrides is clearly anisotropic. Nevertheless they are probable. The of the electron free path length in TiN (according to the data of Tsai et al.[150]) is 39–96 nm (Table 6); according to Krasnosvobodtsev et al.,[138] $\lambda > 40$ nm for stoichiometric NbC films. Unfortunately, the available information about other electrical characteristics (Hall parameters, magnetic resistance, thermo-e.m.f., etc.) for IP

films is limited and is restricted to data for TiN,[129, 153] HfN,[133] and FeTiH.[154]

b. Optical properties

Data on the optical properties of IP are important for decorative applications and also for the construction of devices for the direct conversion of energy. It is well known that in the region of homogeneity titanium nitrides have different colours: $TiN_{\sim 0.5}$ is metallic grey, $TiN_{\sim 0.8}$ is bright yellow, $TiN_{\sim 0.95-0.97}$ is golden yellow, and $TiN_{1.0}$ is brown; carbon and oxygen impurities lead to the blackening and the appearance of a blue tint in the specimens. The optical properties of nitride films have been analysed in reviews on the basis of their electronic structures.[22, 84] The change in optical properties on passing from yttrium dihydride to the trihydride is beautifully illustrated by experiments described by Huiberts et al.[146] and showing that the change in the hydrogen composition of the films is accompanied by a transition from mirror reflection (metal-like $YH_{<2}$) to transparency (nonmetallic $YH_{>2}$) (see also the resistivity ρ in Table 5).

The characteristics of the optical properties of nitride films are presented in Table 7. It is seen that the influence of deviations from stoichiometry is fairly appreciable. The effects associated with the influence of impurities and surface roughness have been analysed.[55, 156] For ZrN film containing 10 at.% of oxygen, the refractive index proved to be 2.15–2.25.[55] The optical properties of TiN_xO_y films obtained by the DCMRS method on architectural glass have been analysed by Polato et al.[157] It has been proposed that the stoichiometry of TiN films be monitored *in situ* on the basis of spectroscopic ellipsometric measurements.[158]

Table 7. Optical properties of nitride films.

Nitride	Forbidden band width /eV	Refractive index [a]	Reflectance (%)[b]	Ref.
Zr_3N_4	2.2	2.9–3.3		55
Hf_3N_4	2.7	2.4–2.8		55
VN		1.5–1.7		56
Nb_3N_4		1.5–2.7		56
Ta_3N_5	2.7	3.0–3.1		56
$TiN_{\sim 1.0}$			0.13	57
$TiN_{\sim 1.0}$			0.20	73
$TiN_{0.67}$			0.45	73
$TiN_{1.04}$			0.1	155
$TiN_{0.95}$			0.15	155
$TiN_{0.8}$			0.35	155
$TiN_{0.52}$			0.45	155

[a] Determined with the aid of an ellipsometer (wavelength 622.8 nm).
[b] Photon energy 2.8 eV.

Boride films are also promising for decorative applications. LaB_6 films have a characteristic violet colour, while ZrB_2 is silver-grey. On doping with nitrogen, the refractive index of the latter remains constant over a wide range of wavelengths and they are extremely corrosion resistant.[77]

2. Hardness

There is no doubt that the measurement of hardness is one of the most popular methods for the investigation of the properties of films, since it is readily accessible and yields much information. However, an unambiguous interpretation of the results obtained by this method is not simple in many instances owing to the high structural sensitivity of hardness and its dependence on the method of measurement and the influence of the load, the film thickness, and the nature of the support. It is difficult to compare the absolute values of hardness and they require a careful analysis. The result of the measurement of the hardness of IP films have been discussed in a number of studies (see, for example, Refs 22–28, 76, 77, 95, 96, 114, 129, 130, and 159–164). We shall consider them for the most thoroughly investigated titanium nitride.

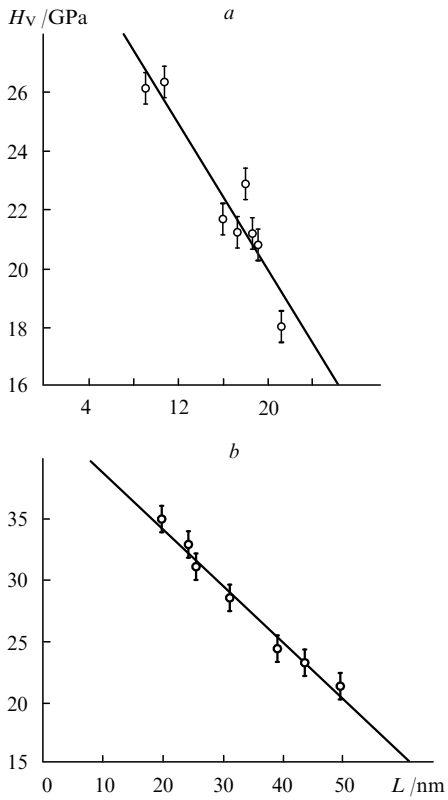


Figure 16. The influence of grain size on hardness.
(*a*) 1 N load; film thickness 20–25 μm; support — Ti–6Al–4V alloy;[95]
(*b*) 0.025 N load; film thickness 1–1.5 μm; substrate — stainless steel.[130]

The influence of various factors on the hardness of TiN films is illustrated in Figs 16–18. Much attention has been devoted [95, 129, 130] to the attestation of the objects of study and the results of these investigations are fully reliable. The familiar Hall–Petch relation, linking hardness (strength) to grain size, holds quite well for films obtained by the AVID method (Fig. 16). Admittedly, it has been noted [95] that, together with the change in grain size, the nitrogen content and the residual stresses also changed in the films (Fig. 17) and the change was nonmonotonic.

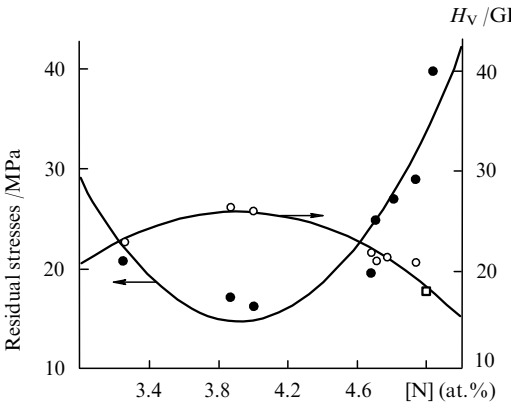


Figure 17. Variation of hardness and residual compressive stresses in the region of homogeneity of TiN.[95]
For conditions, see Fig. 16*a*.

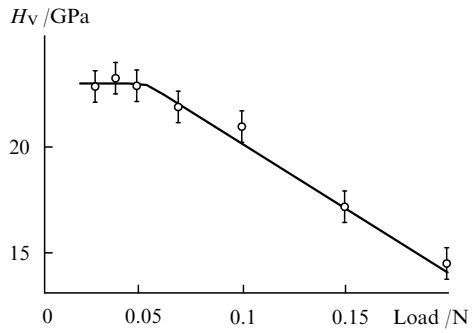


Figure 18. The influence of the load on the hardness of the (111) face of a single-crystal TiN film.[129]
Thickness 2 μm; substrate — MgO single crystal.

Thus, the relation presented in Fig. 16*a* reflects the combined influence of such factors on the hardness of the films. The results for the variation of hardness in the region of homogeneity of TiN agree with the latest data published on this question.[16, 82] It is important to stress that the relations presented in Fig. 16 have been obtained for different loads in the tests (the usual Vickers method[95] and nanoindentation.[130]). The dimensional effect (the influence of the load) is illustrated in Fig. 18, where data for an ideal single crystal TiN film are presented. We may note, however, that certain data of the above studies[95,130] do not agree with the results of other investigations, (for example, of the influence of residual stresses[83]). The overall level of film hardness[95] does not appear very high, which is probably associated with the nature of the support and the thickness of the films in these experiments (in the discussion of the data in Table 3 above, we have already emphasised the uncertainty in the determination of *L*).

It follows from the foregoing that the treatment of the results of the measurement of hardness is not quite so simple. We endeavoured to collect information about the hardness of IP films and attached to them data on the conditions of preparation and measurement (Table 8). Some of the tabulated results have been estimated by means of the relation proposed by Jonsson and Hogmark.[159] Modelling of the hardness of films on supports as the hardness of composites in many cases leads to entirely reasonable results. The values of Knoop hardness are as a rule lower than those of Vickers hardness. The following comments are useful for a correct interpretation of the data presented in Table 8.

1. The methods and deposition regimes employed exert a considerable influence on the hardness of the films.[77, 79, 129, 130, 169, 173, 178, 188] The deposition temperature, the shift potential, the characteristics of the ions, the temperature of the subsequent annealing, and other parameters affect the structures of the films and determine their hardness. The results[178, 188] for TiC–NiB_2 and $Ti(B,N)_x$ films are especially striking in this respect. In the first case, there is a considerable difference between the amorphous and crystalline states (it is not the same for individual compounds and their mixtures). For the boridonitride film, an increase in deposition temperature from 20 to 400 °C also led to an almost twofold increase in hardness. The lower hardness of ZrB_2 and Zr(B,N) films compared with that of titanium diboride and nitridoboride films is also striking. The addition of nitrogen to the former led to the disappearance of the fine columnar structure and the formation of hexagonal boron nitride with a low hardness and effective lubricating properties, which led to an appreciable increase in wear resistance.[77]

2. As a rule, AVID regimes lead to higher hardness parameters compared with other methods. Thus, at the optimum nitrogen pressure and temperature of the support, the hardness of Ti_2N and TiN was respectively ~46.5 and ~42 GPa (load 0.5 N, film thickness 4–6 μm).[189, 190] The influence of nitrogen pressure on hardness, lattice period, and half-height peak width of the (111) reflection is illustrated in Fig. 19 for TiN, (TiZr)N, ZrN, and

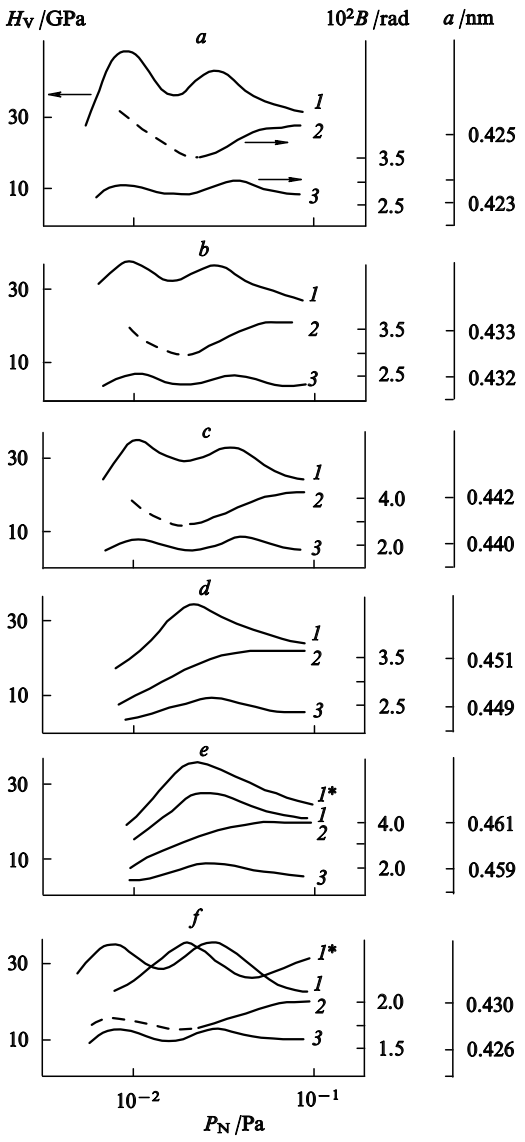


Figure 19. Dependence of hardness (*1*), lattice parameters (*2*), and width of the (111) reflection (*3*) on the nitrogen pressure.[190]
(*a*) TiN; (*b*) (Ti–25 mass% Zr)N; (*c*) (Ti–50 mass%, Zr)N; (*d*) (Ti–75 mass% Zr)N; (*e*) ZrN; (*1**) (Zr–2 mass% Nb)N; (*f*) (Ti–21 mass% Mo)N, (*1**) (Ti–31 mass% Mo)N.

(Ti,Mo)N films. It is striking that cubic titanium nitride which has not yet attained the stoichiometric composition has the maximum hardness. The introduction of dopants into TiN (up to 50%) does not alter the general characteristics (Figs 19*b* and 19*c*), but films with a higher content of zirconium (Fig. 19*d*) as well as films of ZrN itself (Fig. 19*e*) are characterised by a single maximum in the relations presented, because the Zr_2N phase is absent from the Zr–N_2 system. The situation is more complex for (Ti,Mo)N films — in the presence of 21 mass% of Mo it resembles that for weakly doped (Ti,Zr)N films, while a body-centred cubic metallic phase appears for 31 mass% of Mo in the structure and low nitrogen contents.

3. Certain results presented in Table 8 have been obtained in nanoindentation experiments, i.e. for small loads under the conditions of continuous indentation (see, for example, Refs 130, 165, 167, and 168). These data may be somewhat lower than the usual results as a consequence of the influence of the relaxation effect, despite the fact that the influence of the support and of the load is eliminated under nanoindentation conditions (Fig. 18) and this tends to increase the results of the determination

Table 8. Hardness of IP films.

Film	Method of preparation	Thickness / μm	Load / N	Support [a]	Hardness / GPa [b]	Ref.
Nitrides						
$TiN_{1.0}$	AVID (filtered)	20 – 25	1	Ti – 6Al – 4V	17.6±0.9	95
$TiN_{0.87}$	"	20 – 25	1	Ti – 6Al – 4V	21.2±0.5	95
$TiN_{0.66}$	"	20 – 25	1	Ti – 6Al – 4V	25.6±0.8	95
$TiN_{0.48}$	"	20 – 25	1	Ti – 6Al – 4V	22.4±0.9	95
TiN_x	HFMRS	1.8 – 2.5	0.1	RS	~34.3	110
TiN_x	"	4.8	0.15	RS	(~31.2)	111
(111)$TiN_{\sim 1}$	DCMRS	2	0.03 – 0.05	(111)MgO	22.6±0.2	129
$TiN_{\sim 1.0}$	AVID (filtered)	1 – 1.5	0.025	SS	34.4	130
$TiN_{1.0}$	DCMRS	5	0.01 – 0.03	SS	~24	165
$TiN_{0.86}$	"	5	0.01 – 0.03	SS	~28	165
$TiN_{0.55}$	"	5	0.01 – 0.03	SS	31 – 32	165
$TiN_{1.53}$	IBT	0.3	0.25	SS	~30	166
$TiN_{0.9}$	"	0.3	0.25	SS	~35	166
$TiN_{0.47}$	"	0.3	0.25	SS	~27.3	166
$TiN_{0.95}$	PVD(T = 500 °C)	5	0.025	HA	32.4±3.7	167
ZrN_x	AVID	2 – 3	0.5	SS	(26 – 32)	168
ZrN_x	"	2	0.5	HA	27±2	169
HfN_x	"	2 – 3	0.5	SS	(26 – 32)	168
(100)VN_x	DCMRS	2.5	0.08	(100)MgO	~15.9±0.2	170
NbN_x	AVID	2	0.5	HA	34±2	169
CrN_x	"	2	0.5	HA	23±2	169
MoN_x	DCMRS	5 – 20	0.5	SS	35	171
(100)$Ti_{0.5}V_{0.5}N_x$	"	2.5	0.08	(100)MgO	20±0.3	170
$Ti_{0.5}V_{0.5}N_x$	AVID	~5	0.5	RS	~32	172
$Ti_{0.25}V_{0.75}N_x$	"	~5	0.5	RS	~44	172
$Ti_{0.5}Al_{0.5}N_x$	DCMRS	3	0.1	SS	41±9.8	173
$Ti_{0.7}Zr_{0.3}N_x$	"	5	0.5	HA	~33	174
(Ti,Al,Zr)N [c]	"	5	0.5	HA	34.3	72
Carbides						
TiC_x	CVD	6.5	0.025	HA	38.9±6.0	167
TiC_x	AVID (700 °C)	5 – 7	0.5	RS	39.3	175
	(600 °C)	5 – 7	0.5	RS	36.2	175
$TiC_{\sim 0.85}$	CVD	15	0.5	HA	~39	176
$Ti(C_{0.86}O_{0.14})_{1.04}$	IBT	1.5	0.1	(111)Si	(28.2)	177
TiC_x	DCMNS	5	0.5	HA	33.3	178
TiC_x(amorphous)	"	5	0.5	HA	24.5	178
TaC_x	CVD	8	0.5 – 3.9	Tantalum	14.6 [e]	179
$MoC_{0.82}$	DCMRS	5 – 20	0.5	SS	30	171
$W(C_{0.93}O_{0.07})_{1.1-1.2}$	HFMRS	7	0.01	SS	31	180
WC_x	"	5	0.15	RS	45.5	181
WC_x + Co	"	4.5	0.15	RS	20 – 39	181
TiC_xN_y	CVD	3	0.025	HA	30.8±3.1	167
$TiC_{0.5}N_{0.5}$	AVID (600 °C)	5 – 7	0.5	RS	26	175
$TiC_{0.2}N_{0.8}$	"	5 – 7	0.5	RS	25.5	175
$Ti_{0.7}Zr_{0.3}C$	DCMRS	5	0.5	HA	45	174
Borides						
$TiB_{\sim 2}$	DCMNS	5	0.5	HA	34	182
$TiB_{\sim 2}$ (amorphous)	"	5	0.5	HA	23.5	178
$TiB_{\sim 2.8}$	"	4.1	0.15 – 0.30	HA	51	183
$TiB_{\sim 2}$	HFMNS	5	0.25	SS	37.2	184
$TiB_{\sim 1.9}$	DCMNS	~8	0.5	RS	~62.5	185
$TiB_{\sim 2}$	IBT	1	0.25 – 0.75	HA	27.5 [e]	186
$Ti(B,O,N,C)_{2.5}$ [c]	DCMNS	1.8	0.5	(100)TiB_2	44.7±4, 51 [e]	76
$ZrB_{\sim 2}$	"	5	0.2	SS	21.6	187
$YB_{6.5-7.5}$	"	2 – 5	0.1	SS	17 – 18	77
$LaB_{6.5-7}$	"	2 – 5	0.1	SS	10 – 29	77
$SmB_{6.5-7}$	"	2 – 5	0.1	SS	16 – 20	77
$CeB_{7-7.5}$	"	2 – 5	0.1	SS	15 – 22	77
$TiB_{1.6}N_{0.6}$	DCMRS	4.9	0.15 – 0.30	HA	57	183
$TiB_{2.1}N_{0.6}$	"	5	0.5	RS	41.5	185

Table 8 (continued).

Film	Method of preparation	Thickness / μm	Load / N	Support [a]	Hardness / GPa [b]	Ref.
Borides						
$TiBN_{0.4}$	HFMNS					
	20 °C	1–3	(100 nm) [d]	RS	~30	188
	400 °C	1–3	(100 nm) [d]	RS	55	188
$TiB_{1.8}C_{0.5}$	DCMRS	2.7	0.15–0.30	HA	43	183
$TiB_2C_{0.4}N_{0.4}$	"	4.9	0.1–0.30	HA	50	183
$Zr(B,N)_x$	"	2–5	0.1	SS	5–20	77

[a] Supports: RS — rapidly rusting steel; SS — stainless steel; HA — hard alloy. [b] Vickers hardness; the numerals in brackets represent the Knoop hardness. [c] See also Table 2. [d] Depth of penetration by the indentor. [e] Estimated by the method proposed in the study of Jonsson and Hogmark.[159]

of hardness. Yet another characteristic feature of nanoindentation is possible additional scatter of the results associated with the influence of the roughness of the surface (Figs 10–13)

4. A series of data confirm the Hall–Petch relations as regards films (see Fig. 16 and Miura et al.[191]), but this problem does not appear to have been exhausted, particularly in view of the need for a detailed structural and other attestation of the films. For example, the nanoindentatlon of TiN CVD films,[192] deposited on a silicon single crystal at 350 °C, yielded a hardness of 12.7 GPa for a grain size of ~10 nm. This 'record breaking' minimal result (see also Gao et al.[50]) requires an explanation. A series of data on WC films [180, 181] also need interpretation.

5. Alloying is accompanied by an increase in hardness, which has been observed for (Ti,Al)N, (Ti,V)N, (Ti,Nb)N, (Ti,Zr)N, and (Ti,Zr)C films. The presence of oxygen leads as a rule to a decrease in hardness. The influence of nitrogen and carbon atoms is approximately additive. When (Ti,Zr)N and (Ti,Zr)C films are annealed, the spinodal decomposition in the TiN–ZrN and TiC–ZrC systems leads to the formation of a nanocrystalline two-phase structure with a high hardness.[169, 174] This is clearly seen as regards the influence of the annealing temperature on the hardness of doped and multilayer films based on TiN (Fig. 20). The anomalous behaviour of (Ti,Zr)N films is evident.

These data also demonstrate the advantage of multilayer films compared with monolayer and doped films. Composite or multilayer films (they are also referred to as superlattices) have recently attracted much attention.[96, 182, 193] Their high hardness and wear-resistance characteristics have been demonstrated in relation to films in a series of systems: TiC–TiB_2, SiC–TiC, B_4C–TiB_2,[182, 193, 194] TiN–ZrN, TiN–NbN, TiN–CrN,[85, 169, 195] Ti–VN, TiN–NbN, TiN–(Ti, Nb)N,[96, 170] TiN–Si_3N_4,[196] and TiN–CN_x.[197] The technological prospects for the combination of CVD and PVD layers have been discussed.[198]

Figure 21 illustrates the variation of the hardness of multilayer TiN–ZrN, TiN–NbN, and TiN–CrN films with increase in the number of layers (the overall thickness of all the films was the same and amounted to 2 μm). It is possible to specify at least four factors responsible for the increase in hardness with increase in the number of layers (with decrease in their thickness): the increase in the number of interfaces preventing the propagation of dislocations and cracks; the decrease in grain size in individual layers with decrease in their thickness; the increase in the density of noncorrespondence dislocations and the possible more favourable situation as regards residual stresses in the case of multilayer structures. The nonmonotonic variation of hardness in the case of TiN–CrN films may be attributed to the formation of (Ti,Cr)N solid solution and hence to the disappearance of interfaces, which has been confirmed by X-ray phase studies. The formation of a limited amount of solid solutions has also been detected for TiN–NbN and TiN–ZrN films even for the maximum number of layers (180) and individual nitrides continued to be detected by the XRD method. This confirms the major role of interfaces. The reasons for the high hardness of multilayer films have also been discussed in reviews.[28, 96] Attention has been turned to the appreciable difference between the elastic properties of the layers in superlattices.

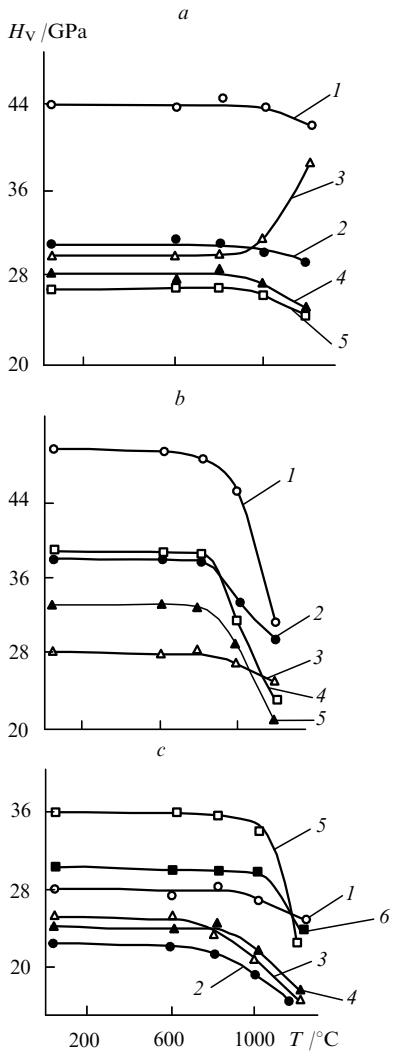


Figure 20. The influence of annealing temperature on the hardness of monolayer (TiN, ZrN, NbN, CrN, Cr_2N), multilayer (TiN–ZrN, TiN–NbN, TiN–CrN), and alloyed [(Ti, Zr)N, (Ti,Nb)N, and (Ti,Cr)N] films.[169]
a: (*1*) TiN–ZrN, 20 layers; (*2*) TiN–ZrN, 10 layers; (*3*) (Ti,Zr)N; (*4*) TiN; (*5*) ZrN; *b*: (*1*) TiN–NbN, 20 layers; (*2*) TiN–NbN, 10 layers; (*3*) TiN; (*4*) NbN; (*5*) (Ti,Nb)N; *c*: (*1*) TiN; (*2*) CrN; (*3*) Cr_2N; (*4*) (Ti,Cr)N; (*5*) TiN–CrN, 20 layers; (*6*) TiN–CrN, 10 layers.

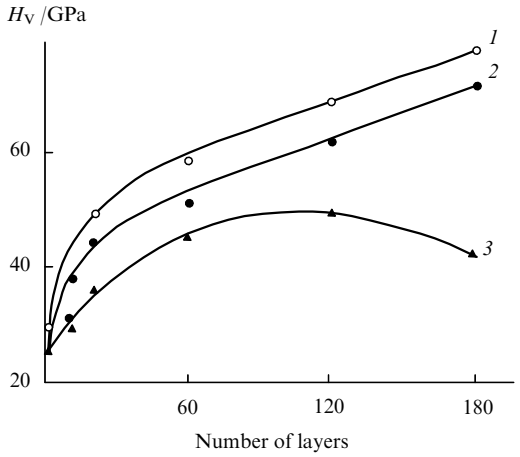


Figure 21. Dependence of the hardness of multilayer nitride films on the number of layers.[85]
(*1*) TiN – NbN; (*2*) TiN – ZrN; (*3*) TiN – CrN.

It is of interest that after some time (possibly several months, which could not unfortunately be established) the high hardness of the TiN – NbN and TiN – ZrN films vanished, evidently as a consequence of the diffusional dissipation of the individual layers.[85] The existence of relaxation effects in multilayer nitride films has also been noted by Hultman et al.[108] The problem of the stability of multilayer structures over a wide temperature range requires separate study.

The short-term high-temperature hardness of TiN, HfN, ZrN, (Ti,Al)N, and TiC – TiB_2 films has been investigated at temperatures up to 1000 °C.[178, 199] Whereas the hardnesses of nitride films differ insignificantly up to 1000 °C (8 – 10 GPa), the difference for TiC, TiB_2, and TiC – TiB_2 films is more significant (for example, at 900 °C it amounts to ~20 GPa for NiB_2 – 20% TiC and ~9 GPa for TiB_2 – 50% TiC). It may be that this situation is due to the manifestation of high-temperature superplasticity in two-phase equimolar mixtures, which was observed in experiments on creep for these and other two-phase compositions based on refractory compounds (see, for example, Refs l6, 32, and 33).

It must be emphasised that the knowledge of hardness is useful for correlation with numerous properties important in the practical employment of the films. Such characteristics are determined in tests of the specimens for wear resistance, for microscratching in the study of the adhesion of the films and coatings, and for microbrittleness and cracking resistance in the modelling of disintegration under a concentrated load, etc. (see, for example, Refs 16, 24, 25, 200, and 201). However, these processes will not be considered here.

3. Other characteristics

Table 9 presents data on the elastic properties. In the analysis of these results, one should bear in mind that the absolute values of the elastic properties are influenced not only by the method of preparation, which determines the structure, texture, composition, and size of the specimens, but also by the method of measurement (see, for example, the relevant reviews [164, 165]). For stoichiometric TiN and ZrN, the results of Torok et al.[202] are the most representative. They agree well with the results of the study of Portnoi et al.[208] obtained on analogous nonporous nitride

Table 9. The normal moduli of elasticity (*E*), moduli of shear (*G*), and Poisson coefficients (*v*) for IP films.

Film	Method of preparation	Method of measurement [a]	Thickness / μm	Texture	*E* / GPa	*G* / GPa	*v*	Ref.
Nitrides								
$TiN_{1.0}$	DCMRS	1	4 – 6	< 220 >	637	–	–	202
$TiN_{0.5-1.0}$	"	2	5	–	300 – 450	–	–	165
TiN_x	"	3	5	< 311 >, < 200 >		–	0.30	203
$TiN_{0.97}$	"	2	0.2 – 1	< 111 >	550±50	–	–	204
$TiN_{\sim 0.8}$	IBT	2	0.3 – 0.9	–	~450	–	–	205
$TiN_{\sim 0.8}$	"	4	0.3 – 0.9	–	–	~130	–	205
$TiN_{0.8}$	HFMRS	2	1 – 3	–	410	–	–	188
TiN_x	DCMRS	4	2	–	–	~192	–	206
TiN_x	AVID	2	2	–	370±81	–	–	207
$ZrN_{\sim 1.0}$	DCMRS	1	4 – 6	< 111 >	460	–	–	202
ZrN_x	"	3	5	< 200 >, < 111 >	–	–	0.19	203
$HfN_{\sim 1.0}$	"	1	4 – 6	< 311 >	380	–	–	202
HfN_x	"	3	5	< 311 >, < 111 >	–		0.35	203
VN_x	"	4	2	–	–	~149	–	206
NbN_x	"	4	2	–	–	~142	–	206
$(V,Nb)N_x$	"	4	2	–	–	~124	–	206
$(Ti,Al)N_x$	AVID	2	2	–	298±72	–	–	207
$(Ti,Nb)N_x$	"	2	2	–	375±43	–	–	207
Carbides								
$TiC_{\sim 1.0}$	DCMRS	1	4 – 6	< 111 >	460	–	–	202
$Ti(C,N)_x$	AVID	2	2	–	300±30	–	–	207
Borides								
$TiB_2N_{0.6}$	HFMNS	2	1 – 3	–	640	–	–	188
$TiB_{1.4}N_{0.5}$	"	2	1 – 3	–	750	–	–	188
$TiBN_{0.4}$	"	2	1 – 3	–	500	–	–	188
$TiB_{0.7}N_{0.5}$	"	2	1 – 3	–	453	–	–	188
$TiB_{0.6}N_{0.5}$	"	2	1 – 3	–	276	–	–	188

[a] Methods of measurement: (1) resonance bending vibrations; (2) nanoindentation (3) X-ray studies; (4) Brillouin scattering.

specimens prepared by the method involving, the through-saturation of the metals with nitrogen.

The nanoindentation method, involving the analysis of the form of the load-release curve, has come to be widely used in the study of elastic properties (as in the study of hardness). However, not all the results obtained by this method (for example, the data of Vancoille et al.[207]) have been reasonably interpreted. The high values of the modules of elasticity (E) for certain boridonitride films are also noteworthy.[188] It is likewise of interest that the decrease in the deposition temperature from 400 to 20 °C led to a decrease in E by a factor of almost 1.5 ($TiBN_{0.5}$). It has been noted [207] that annealing of the films leads to an increase in their modulus of elasticity, but above 500 °C it diminishes. In the study of multilayer films, anomalies in elastic properties were not observed for the TiN–(V,Nb)N system, in contrast to hardness.[209]

The tribological and corrosion properties of IP films [24, 25, 77, 111, 113, 115, 198, 210–215] have been the subject of numerous investigations. At the same time, problems such as those of phase equilibria and the thermodynamic, thermal, and diffusion properties have been studied to an extremely limited extent in relation to IP films.[32, 33, 216] So far as we are aware, the available information about diffusion is limited to studies on films as barrier layers (see, for example, Ostling et al.[217] and Shin et al.[218]). The thermodynamic properties and phase equilibria have been investigated for certain hydride films [$VH(D)_x$ and PdH_x].[219, 220] In particular, a change in the nature of the isotherms and a decrease in the critical point for decomposition have been noted in the palladium–hydrogen system for films ~50 nm thick as a possible result of the influence of nanocrystallinity on the equilibrium in this system (for films 300 nm thick, anomalies were not observed).[220] On the other hand, for vanadium films 500 nm thick and with a grain size of ~50 nm, measurements of the partial and integral thermodynamic properties revealed no differences relative to the usual polycrystalline vanadium on interaction with hydrogen.[219] The emission characteristics of lanthanide boride films are discussed in a review.[77]

The thermal stabilities and the recrystallisation of IP films have been studied by a series of investigators (see, for example, Refs 93, 169, 174, 195, 199, 207, and 221–223). It is well known that the formation of a granular structure and recrystallisation begin even during the deposition of the films. Fig. 22 illustrates the influence of film thickness on the grain size for various nitrides. There is an evident difference between ZrN, on the one hand, and TiN, NbN, and CrN, on the other. It may be that this is associated with the greater affinity of zirconium for nitrogen and

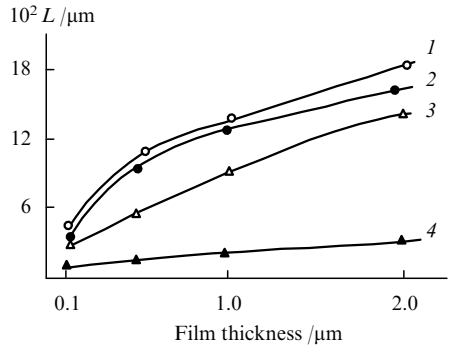


Figure 22. Dependence of grain size on the thickness of the films.[223] (*1*) TiN; (*2*) CrN; (*3*) NbN; (*4*) ZrN.

Table 10. The grain sizes in nitride films 2 μm thick obtained by the AVID method.[223]

Film	Grain size/ μm			Energy of mixing in (Ti, M)N system / kJ mol^{-1}
	I	II	III	
TiN	0.18±0.08			
CrN	0.16±0.08	0.17±0.05	0.18±0.04	3.4
NbN	0.14±0.03	0.04±0.01	0.08±0.02	6.1
ZrN	0.03±0.02	~0.01	0.02±0.01	32.6
AlN	0.15±0.05	0.08±0.03	~0.01	37.2

Note. The following designations have been adopted: (I) unalloyed film; (II) multilayer TiN–MN film (10–20 layers); alloyed (Ti,M)N film.

the higher energy of zirconium ions. It is of interest that the smallest grains are observed also in multilayer and doped films with ZrN (Table 10). This is also correlated with the high energy of mixing in the TiN–ZrN system. The latter characteristic is known to be related to the diffusional and recrystallisation mobilities.

The influence of film thickness, alloying, and multilayer structure on the recrystallisation of a series of nitrides has been investigated in a number of studies.[169, 195, 221, 223] Fig. 23 illustrates this in relation to TiN and NbN. The recrystallisation of TiN and NbN begins at virtually identical temperatures, although a greater spread in size is characteristic of TiN. It is also evident that thinner films recrystallise more intensely, but in multilayer and doped structures this process is retarded, especially in the case of TiN–ZrN and (Ti,Zr)N (Table 10). Many details and the mechanism of the high-temperature behaviour of IP films require additional studies.

V. Conclusion

The available information about IP films is diverse but inhomogeneous. Most of it refers to nitrides and, in particular, to TiN. Much less is known about carbides and hydrides, borides occupying an intermediate position. However, so far as one can judge from the problems dealt with in the latest symposia on borides (Austria, August, 1996) and hydrides (Switzerland, August, 1996), there is a growing interest in boride and hydride films. The reactivity and catalytic properties of thin carbide and nitride layers are also being comprehensively investigated.[224] In the present review, the author, whilst not claiming to examine all the problems of film IP, has endeavoured to emphasise certain unsolved problems and in this connection the available information about the structures and physicochemical properties of these objects appears far from complete. For example, the data on the structures of the interfaces for IP films are greatly inferior to those for metals.[225] It is thought that the accumulation of new fundamental results for IP films will promote the development of the physicochemical foundations of the nanostructural materials science and the expansion of the range of their diverse applications.

This review has been written within the framework of projects supported by the Russian Fundamental Research Fund (grant No. 95-02-03518) and the INTAS program (grant No. 94-1291).

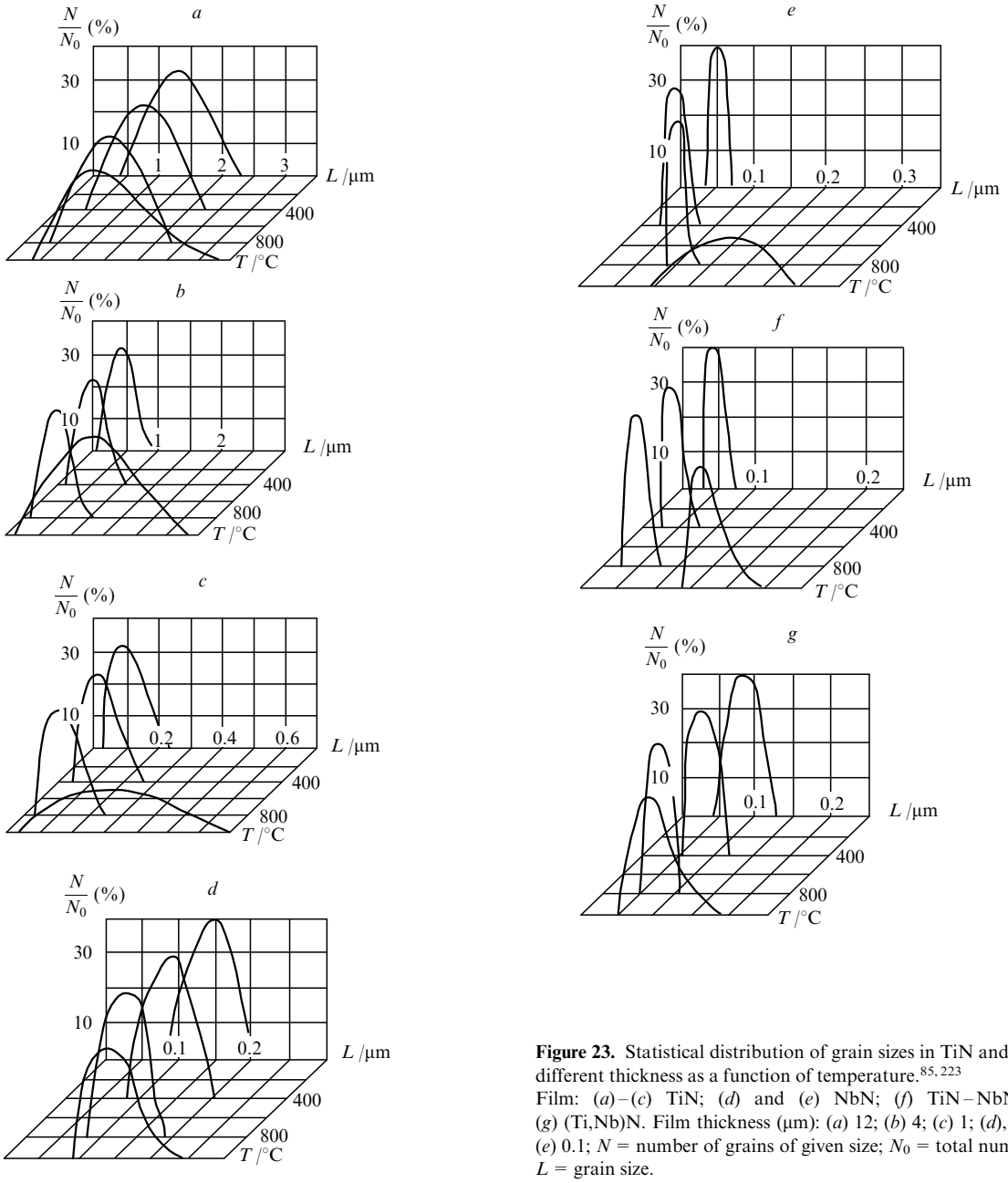


Figure 23. Statistical distribution of grain sizes in TiN and NbN films of different thickness as a function of temperature.[85, 223]
Film: (*a*)–(*c*) TiN; (*d*) and (*e*) NbN; (*f*) TiN–NbN, 20 layers; (*g*) (Ti,Nb)N. Film thickness (μm): (*a*) 12; (*b*) 4; (*c*) 1; (*d*), (*f*), and (*g*) 2; (*e*) 0.1; N = number of grains of given size; N_0 = total number of grains; L = grain size.

References

1. G Hagg *Z. Phys. Chem.* **B12** 33 (1931)
2. R A Andrievskii, Ya S Umanskii *Fazy Vnedreniya* (Interstitial Phases) (Moscow: Nauka, 1977)
3. G V Samsonov, Ya S Umanskii *Tverdye Soedineniya Tugoplavkikh Metallov* (Solid Compounds of Refractory Metals) (Moscow: Metallurgiya, 1957)
4. H J Goldschmidt *Interstitial Alloys* (New York: Plenum, 1967)
5. E K Storms *The Refractory Carbides* (New York: Academic Press, 1967)
6. G V Samsonov *Nitridy* (The Nitrides) (Kiev: Naukova Dumka, 1969)
7. L E Toth *Transition Metal Carbides and Nitrides* (New York: Academic Press, 1971)
8. G V Samsonov, V S Neshpor, G S Upadkhaya *Fizicheskoe Materialovedenie Karbidov* (Physical Materials Science of Carbides) (Kiev: Naukova Dumka, 1974)
9. Yu V Levinskii *Diagrammy Sostoyaniya Metallov s Gazami* (Phase Diagrams of Metals with Gases) (Moscow: Metallurgiya, 1975)
10. A A Smirnov *Teoriya Splavov Vnedreniya* (Theory of Interstitial Alloys) (Moscow: Nauka, 1979)
11. Yu B Kuz'ma *Kristallokhimiya Boridov* (Crystal Chemistry of Borides) (Lvov: Vyshcha Shkola, 1983)
12. H Holleck *Binare und Ternare Carbid- und Nitridsysteme der Ubergangsmetalle* (Berlin: Gebruder Borntrager, 1984)
13. G P Shveikin, S I Alyamovskii, Yu G Zainulin, A I Gusev *Soedineniya Peremennogo Sostava i ikh Tverdye Rastvory* (Compounds of Variable Composition and Their Solid Solutions) (Sverdlovsk: Ural Branch of the Academy of Sciences of the USSR, 1984
14. P V Zubarev *Zharoprochnost' faz Vnedreniya* (High Resistance of Interstitial Phases) (Moscow: Metallurgiya, 1985)
15. R A Andrievskii *Materialovedenie Gidridov* (Materials Science of Hydrides) (Moscow: Metallurgiya, 1986)
16. R A Andrievskii, I I Spivak *Prochnost' Tugoplavkikh Soedinenii i Materialov na Ikh Osnove* (Strength of Refractory Compounds and Materials Based upon Them) (Chelyabinsk: Metallurgiya, 1989)

17. E A Zhurakovskii, V F Nemchenko *Kineticheskie Svoistva i Elektronnaya Struktura Faz Vnedreniya* (The Chemical Properties and Electronic Structure of Interstitial Phases) (Kiev: Naukova Dumka, 1989)
18. E I Serebryakova, V A Neronov, P D Peshev *Vysokotemperaturnye Boridy* (High-Temperature Borides) (Moscow: Metallurgiya, 1991)
19. A I Gusev *Fizicheskaya Khimiya Nestekhiometricheskikh Tugoplavkikh Soedinenii* (Physical Chemistry of Nonstoichiometric Refractory Compounds) (Moscow: Nauka, 1991)
20. A A Rempel' *Effekty Uporyadocheniya v Nestekhiometricheskikh Soedineniyakh Vnedreniya* (Ordering Effects in Nonstoichiometric Interstitial Compounds (Ekaterinburg: Nauka, 1992)
21. V A Gubanov, A L Ivanovskiy, V P Zhukov *Electronic Properties of Refractory Carbides and Nitrides of the Transition Metals* (Cambridge: Cambridge University Press, 1994)
22. J-E Sundgren *Thin Solid Films* **128** 21 (1985)
23. K Reichelt, X Jiang *Thin Solid Films* **191** 91 (1990)
24. D S Rickerby, A Matthews *Rev. Powder Metall. Phys. Ceram.* **4** 155 (1991)
25. S Chatterjee, T S Sudarshan, S Chandrashekhar *J. Mater. Sci.* **28** 1989 (1993)
26. J Musil, J Vyskocil, S Kadlec, in *Physics of Thin Films. Mechanic and Dielectrical Properties* Vol. 17 (Eds M H Francombe, J L Vossen) (New York: Academic Press, 1993) p. 79
27. H Rebenne, D G Bhat *Surf. Coat. Technol.* **63** 1 (1994)
28. J-E Sundgren, L Hultman, in *Materials and Processes for Surface and Interface Engineering* (Ed.Y Pauleau) (Dordrecht: Kluwer Academic, 1995) p. 453
29. A V Belyi, G D Karpenko, N K Myshkin *Struktura i Metody Formirovaniya Iznosostoikikh Poverkhnostnykh Sloev* (The Structure and Methods for the Formation of Wear-resistant Surface Layers) (Moscow: Mashinostroenie, 1991)
30. V V Kudinov, G V Bobrov *Nanesenie Pokrytii Napyleniem. Teoriya, Tekhnologiya i Oborudovanie* (Deposition of Coatings by Spraying. Theory, Technology, and Equipment) (Moscow: Metallurgiya, 1992)
31. M Konuma *Film Deposition by Plasma Technique* (Berlin: Springer, 1992)
32. R A Andrievskii *J. Mater. Sci.* **29** 614 (1994)
33. R A Andrievskii *Usp. Khim.* **63** 431 (1994) [*Russ. Chem. Rev.* **63** 411 (1994)
34. R F Bunshah, R Nimmagadda, W Dunford, B A Movchan, A V Demchishin, A Chursanov *Thin Solid Films* **54** 85 (1978)
35. A I Golovashkin, B G Zhurkin, A L Karuzskii, S I Krasnosvobodtsev, V P Martovitskii, E V Pechen', V V Rodin, Yu I Stepanov, A V Shirkov *Fiz. Tverd. Tela* **28** 3342 (1986)[a]
36. R F Bunshah, C V Deshpandey *J. Vac. Sci. Technol.* **A3** 553 (1985)
37. S K Singh, K Ramakrishna, A K Singh, O N Srivastava *Int. J. Hydrog. Energy* **14** 573 (1989)
38. J Li, Y-T Cheng *J. Alloys Compd.* **223** 6 (1995)
39. D M Mattox, J E McDonald *J. Appl. Phys.* **34** 2493 (1963)
40. A M Dorodnov *Zh. Tekhn. Fiz.* **48** 1858 (1978)[b]
41. H Randhawa *Thin Solid Films* **196** 329 (1991)
42. I I Aksenov, V G Bren', V G Padalka, V M Khoroshikh *Zh. Tekhn. Fiz.* **48** 1165 (1978)[b]
43. P J Martin, R P Netterfield, T I Kinder *Thin Solid Films* **193** 77 (1990)
44. O Knotek, F Lofler, G Kramer *Surf. Coat. Technol.* **59** 14 (1993)
45. B O Johansson, H T G Hentzell, J M E Harper, J J Cuomo *J. Mater. Res.* **1** 442 (1986)
46. Y Genqing, W Dazhi, L Xianghuai, W Xi, Z Shichang *Surf. Coat. Technol.* **65** 214 (1994)
47. J P Riviere, Ph Guesdon, J Delafond, M F Denanot, G Farges, D Degout *Thin Solid Films* **204** 151 (1991)
48. A V Byeli, S A Fedotov *Surf. Eng.* **10** 136 (1994)
49. C I M A Spee, J P A M Driessen, A D Kuypers *J. Phys. IV. Colloq. C5* **5** 719 (1995)
50. L X Cao, Z C Feng, Y Liang, W L Hou, B C Zhang, Y Q Wang, L Li *Thin Solid Films* **257** 7 (1995)
51. H Tsuda, Y Numasawa *Jpn. J. Apll. Phys.* **34** L691 (1995)
52. A Weber, R Nikulski, C-P Klages, M E Gross, W L Brown, E Dons, R M Charatan *J. Electrochem. Soc.* **141** 849 (1994)
53. M Boumerzoug, P Mascher, J G Simmons *Appl. Phys. Lett.* **66** 2664 (1995)
54. A Weber, R Poelckelmann, C-P Klages *Appl. Phys. Lett.* **67** 2934 (1995)
55. R Fix, R G Gordon, D M Hoffman *Chem. Mater.* **3** 1138 (1991)
56. R Fix, R G Gordon, D M Hoffman *Chem. Mater.* **5** 614 (1993)
57. M Ritala, M Leskela, E Rauhala, P Haussalo *J. Electrochem. Soc.* **142** 2731 (1995)
58. H Zheng, K Oka, D Mackenzie, in *Better Ceramics Through Chemistry* Vol. 271 (Eds M J Hampden-Smith, W G Klemperer, C J Brikes) (Pittsburgh, MRS, 1992) p. 893
59. J A Jensen, J E Gozum, D M Pollina, G S Girolami *J. Am. Chem. Soc.* **110** 1643 (1988)
60. A L Wayda, L F Schneemeyer, R L Opila *Appl. Phys. Lett.* **53** 361 (1988)
61. R A Andrievski, S E Kravchenko, S P Shilkin, in *Proceedings of the 11th Internetional Symposium on Boron, Borides and Related Compounds* (Eds R Uno, IHigashi) (JJAP Ser. 10, Tokyo, 1994) p. 198
62. R A Andrievskii, S E Kravchenko, S P Shilkin *Neorg. Mater.* **31** 1048 (1995)[c]
63. Yu A Bykovskii, V N Nevolin, V Yu Fominskii *Ionnaya i Lazernaya Implantatsiya Metallicheskikh Materialov* (Ionic and Laser Implantation of Metallic Materials) (Moscow: Energoatomizdat, 1991)
64. K Yabe, O Nishimura, T Fujihana, M Iwaki *Surf. Coat. Technol.* **66** 250 (1994)
65. Y Kasukabe, J Ootubo, Sh Nagata, M Kishimoto, Y Fuino, S Yamaguchi, Y Yamada *Jpn. J. Appl. Phys.* **34** 3234 (1995)
66. T Shibutami, Y Kanzaki, O Matsumoto *J. Less-Common Met.* **113** 177 (1985)
67. K W Vogt, L A Naugher, P A Kohl *Thin Solid Films* **256** 106 (1995)
68. I P Jain, Y K Vijay, K S Upadhyay, M Singh *Int. J. Hydrog. Energy* **15** 345 (1990)
69. H Sakaguchi, T Tsujimoto, G Adachi *Chem. Mater.* **5** 6 (1993)
70. D P Woodruff, T A Delchar *Modern Techniques of Surface Science* (Cambridge: Cambridge University Press, 1986)
71. J-P Noel, D C Houghton, G Este, F R Shepherd, H Plattner *J. Vac. Sci. Technol.* **A2** 284 (1984)
72. O Knotek, M Bohmer, T Leyendecker, F Jungblut *Mater. Sci. Eng.* **A105**/**106** 481 (1988)
73. P Panjan, B Navinsek, A Zabkar, J Fiser, A Zalar *Vacuum* **40** 81 (1990)
74. R Lohmann, E Osterschulze, K Thoma, H Gartner, W Herr, B Matthes, E Broszeit, K-H Kloos *Mater. Sci. Eng.* **A139** 259 (1991)
75. M Yoshitake, T Yotsuya, S Ogawa *Jpn. J. Appl. Phys.* **31** 4002 (1992)
76. R A Andrievskii, G V Kalinnikov, A F Potafeev, M A Ponomarev, S Yu Sharivker *Neorg. Mater.* **31** 1536 (1995)[c]
77. C Mitterer *J. Solid State Chem.* (1997) (in the press)
78. D V Shtanskii, E A Levashov, V I Kosyanin, N B D'yakonova, I V Lyasotskii *Fiz. Met. Metalloved.* **80** 120 (1995)
79. N Eguchi, V Grajewski, H H Uchida, E Fromm *Mater. Sci. Eng.* **A139** 339 (1991)
80. T P Mollart, M Baker, J Haupt, A Steiner, P Hammer, W Gissler *Surf. Coat. Technol.* **74**–**75** 491 (1995)
81. M Baker, J Haupt, W Gissler *Z. Naturforsch., A, Phys. Sci.* **50** 624 (1995)
82. W Lengauer *J. Alloys Compd.* **186** 293 (1992)
83. V Valdova *J. Alloys Compd.* **219** 83 (1995)
84. A J Perry *J. Vac. Sci. Technol.* **A6** 2140 (1988)
85. R A Andrievskii, I A Anisimova, V P Anisimov *Fiz. Khim. Obrab. Mater.* (2) 99 (1992)
86. R R Manory, G Kimmel *Surf. Coat. Technol.* **63** 85 (1994)
87. J Brunner, A J Perry *Thin Solid Films* **153** 103 (1987)
88. J P Schaffer, A J Perry, J Brunner *J. Vac. Sci. Technol.* **A10** 193 (1992)
89. A Uedono, S Nanao, Sh Tanigawa, R Suzuki, T Ohdaira, T Mikado, Sh Ishibashi *Jpn. J. Appl. Phys.* **34** 5711 (1995)
90. E V Shalaeva, M V Kuznetsov, R S Baryshev, B V Mitrofanov *J. Phys. IV. Suppl.* **1** C 2 (1991)
91. A Laor, L Zevin, J Pelleg, N Croitoru *Thin Solid Films* **232** 143 (1993)
92. N Hayashi, I H Murzin, I Sakamoto, M Ohkubo *Thin Solid Films* **259** 146 (1995)

93. J Chen, J A Barnard *Mater. Sci. Eng.* **A191** 233 (1995)
94. M V Kuznetsov, E V Shalaeva, S V Borisov, B V Mitrofanov, A L Ivanovski, G P Shveikin *Mendeleev Commun.* 94 (1995)
95. J A Sue *Surf. Coat. Technol.* **61** 115 (1993)
96. S A Barnet, in *Physics of Thin Films. Mechanic and Dielectric Properties* Vol. 17 (Eds M H Francombe, J L Vossen) (New York: Academic Press, 1993) p. 1
97. E M Lazarev, S Ya Betsofen *Fiz. Khim. Obrab. Mater.* (6) 60 (1993)
98. C Jiang, T Goto, T Hirai *J. Mater. Sci.* **29** 669 (1994)
99. U C Oh, J H Je, J Y Lee *J. Mater. Res.* **10** 634 (1995)
100. H H Yang, J H Je, K-B Lee *J. Mater. Sci. Lett.* **14** 1635 (1995)
101. I V Aleksandrov, R Z Valiev *Fiz. Met. Metalloved.* **76** 77 (1994)
102. D Wang, X Wang, G Yang, X Liu, Y Jia, G Zhou, G Li *J. Appl. Phys.* **77** 2945 (1995)
103. H Yomoto, K Kaneko, M Ishihara, K Akasi, T Kaneko *Adv. Mater. Opt. Electr.* **5** 191 (1995)
104. V Valdova, J Musil *Thin Solid Films* **149** 49 (1987)
105. D Maheo, J-M Poitevin *Thin Solid Films* **237** 78 (1994)
106. H G Jiang, H Y Tong, K Lu, B Z Ding, Q H Song, Z Q Hu, in *Advanced Materials'93, I/A: Ceramics, Powders, Corrosion, and Advanced Processing* Vol. 14A (Eds N Mizutani et al.) (Amsterdam: Elsevier, 1994) p. 785
107. N B D'yakonova, D V Shtanskii, I V Lyasotskii *Fiz. Met. Metalloved.* **78** 86 (1994)
108. L Hultman, M Shinn, P B Mirkarimi, S Barnett *J. Cryst. Growth* **135** 309 (1994)
109. L Hultman, U Helmersson, S A Barnett, J-E Sundgren, J E Greene *J. Appl. Phys.* **61** 552 (1987)
110. K J Ma, A Bloyce *Surf. Eng.* **11** 71 (1995)
111. I Effoglu, R D Arnell, S F Tinston, D G Teer *Surf. Coat. Technol.* **57** 61 (1993)
112. P Jin, S Nakao, S Tanemura, S Maruno *Thin Solid Films* **271** 19 (1995)
113. E Broszeit, B Matthews, W Herr, K H Kloos *Surf. Coat. Technol.* **58** 29 (1993)
114. R A Andrievskii, in *Fracture Mechanics of Ceramics* Vol. 11 (Eds R C Brandt, D P H Hasselman, D Munz, V Ya Shevchenko) (New York: Plenum, 1996)
115. J Aromaa, H Ronkainen, A Mahiout, S-P Hannula, A Leyland, A Matthews, B Matthes, E Broszeit *Mater. Sci. Eng.* **A140** 722 (1991)
116. A A Babad-Zakhryapin *Defekty v Pokrytiyakh* (Defects in Coatings) (Moscow: Energoatomizdat, 1987)
117. K L Westra, D J Thompson *Thin Solid Films* **257** 15 (1995)
118. K Bartsch, A Leonhardt, E Wolf, M Schonner *J. Mater. Sci.* **26** 4318 (1991)
119. R Hillel, M Maline, F Gourbilleau, G Nouet, R Carles, A Mlayah *Mater. Sci. Eng.* **A168** 183 (1993)
120. Y J Liu, H J Kim, Y Egashira, H Kimura, H Komiyama *J. Am. Ceram. Soc.* **79** 1335 (1996)
121. B A Movchan, A V Demchishin *Fiz. Met. Metalloved.* **28** 653 (1969)
122. J A Tornton *Annu. Rev. Mater. Sci.* **7** 239 (1977)
123. S K Kim, H H Lee *J. Appl. Phys.* **78** 3809 (1995)
124. A L Ivanovskii *Usp. Khim.* **64** 499 (1996) [*Russ. Chem. Rev.* **64** 461 (1996)]
125. A Lebugle, R Nyholm, N Martensson *J. Less-Common Met.* **82** 269 (1981)
126. M V Kuznetsov, S V Borisov, Yu F Zhuravlev, R S Baryshev, O F Denisov, B V Mitrofanov, V A Gubanov *Poverkhnost'* (12) 141 (1989)
127. M V Kuznetsov, Yu F Zhuravlev, D L Novikov, V A Gubanov *Poverkhnost'* (1) 131 (1990)
128. R P Netterfield, P J Martin, D R McKeenzie *J. Mater. Sci. Lett.* **9** 972 (1990)
129. B O Johansson, J-E Sundgren, J E Greene, A Rocekett, S A Barnett *J. Vac. Sci. Technol.* **A3** 303(1985)
130. A Bendavid, P J Martin, R P Netterfield, T J Kinder *Surf. Coat. Technol.* **70** 97 (1994)
131. T Zheleva, S Oktyabrsky, K Jagannadham, R D Vispute, J Narayan *J. Mater. Res.* **11** 399 (1996)
132. S Horita, T Tujikawa, H Akahori, M Kobayashi, T Hata *J. Vac. Sci. Technol.* **A11** 2452 (1993)
133. R Nowak, S Maruno *Mater. Sci. Eng.* **A202** 226 (1995)
134. L Rivaud, S Barnett, J Greene, E Marciniec *J. Vac. Sci. Technol.* **A9** 2180 (1991)
135. K K Shih, D D Dove *J. Vac. Sci. Technol.* **A8** 1399 (1990)
136. F C T So, E Kolawa, X-A Zhao, M-A Nicolet *Thin Solid Films* **153** 507 (1987)
137. J-F Lei, H Okimura, J O Brittain *Mater. Sci. Eng.* **A123** 129 (1990)
138. S I Krasnosvobodtsev, N P Shabanova, E V Ekimov, V S Nozdrin, E V Pechen' *Zh. Eksp. Teor. Fiz.* **108** 970 (1995)[d]
139. J R Shapiro, J J Finnegan *Thin Solid Films* **107** 81 (1983)
140. J G Ryan, S Roberts, G J Slusser, D Adams *Thin Solid Films* **153** 329 (1987)
141. R A Andrievskii, G V Kalinnikov *Fiz. Tverd. Tela* (1997) (in the press)[a]
142. W Y Lee, G Olive, F Sequeda, V Deline, T Huang, G Gorman, D W Chung *Thin Solid Films* **166** 131 (1988)
143. D S Wuu, M L Lee, T Y Lin, R H Horng, in *Thin Film Materials Surface & Interface Structure ULSI Materials* Vol. 1 (Eds L J Chen, T T Tsong, S C Sun) (Taiwan: MRS-Taiwan, 1995) p. 119
144. J G Rjan, S Roberts *Thin Solid Films* **135** 9 (1986)
145. R Spulak *J. Less-Common Met.* **160** 15 (1990)
146. J N Huiberts, R Griessen, J H Rector, R J Wijngaarden, J P Dekker, D G Groot, N J Koeman *Nature (London)* **380** 231 (1996)
147. G Adachi, K Niki, H Nagai, J Shiokawa *J. Less-Common Met.* **88** 213 (1982)
148. H Sakaguchi, Y Yagi, N Taniguchi, G Adachi, J Shiokawa *J. Less-Common Met.* **135** 137 (1987)
149. K H Schwarz, A R Williams, J J Cuomo, J M E Harper, H T G Hentzel *Phys. Rev. B, Condens Matter.* **8** 5489 (1985)
150. W Tsai, M Delfino, J A Fair, D Hodul *J. Appl. Phys.* **73** 4462 (1993)
151. M J Deen *Thin Solid Films* **152** 534 (1987)
152. N Hirashita, J E Greene, U Helmersson, J Birch, J-E Sundgren *J. Apll. Phys.* **70** 4963 (1991)
153. Y Igasaki, H Mitsuhashi *Thin Solid Films* **70** 17 (1980)
154. M Singh *Int. J. Hydrog. Energy* **21** 223 (1996)
155. L Roux, J Hanus, J C Francois, M Sigrist *Sol. Energy Mater.* **7** 299 (1982)
156. M Bonelli, L A Guzman, M Miotello, L Calliari, M Elena, P M Ossi *Vacuum* **43** 459 (1992)
157. P Polato, H Franz, F Rustichelli, M Montecchi, A Piegari *Thin Solid Films* **248** 184 (1994)
158. L Logothetidis, I Alexandrou, A Papadopoulus *J. Appl. Phys.* **77** 1043 (1995)
159. B Jonsson, S Hogmark *Thin Solid Films* **114** 257 (1984)
160. A A Voevodin, S E Spasskii, A L Erokhin *Zavod. Lab.* **57** 45 (1991)
161. S A Betsofen *Metally* (2) 181 (1993)
162. T F Page, V Hainsworth *Surf. Coat. Technol.* **61** 201 (1993)
163. E D Nicholson, J E Field *J. Hard. Mater.* **5** 89 (1994)
164. E Soderlund, D J Rowcliffe *J. Hard Mater.* **5** 149 (1994)
165. W C Oliver, C J McHargue, S J Zinkle *Thin Solid Films* **153** 185 (1987)
166. D C Kothari, P Scardi, S Gialaniella, I Guzman *Phylos. Mag.* **B61** 627 (1990)
167. E Soderlund, D J Rowcliffe, in *Mechanical Properties and Deformation Behaviour of Materials Having Ultra-Fine Microstructure.* (Eds M Nastasi, D M Parkin, H Gleiter) (Dordrecht: Kluwer Academic, 1993) p. 463
168. O A Johansen, J H Dontje, R L D Zenner *Thin Solid Films* **153** 75 (1987)
169. R A Andrievski, I A Anisimova, V P Anisimov *Thin Solid Films* **205** 171 (1991)
170. U Helmersson, S Todorova, S A Barnett, J-E Sundgren, L S Markert, J E Greene *J. Appl. Phys.* **62** 481 (1987)
171. J Danroc, A Aubert, R Gillet *Thin Solid Films* **153** 281 (1987)
172. O Knotek, W Burgmer, C Stoessel *Surf. Coat. Technol.* **54/55** 249 (1992)
173. G Hakansson, J-E Sundgren, D McIntyre, J E Greene, W-D Munz *Thin Solid Films* **153** 55 (1987)
174. O Knotek, A Barimani *Thin Solid Films* **174** 51 (1989)
175. H Randhawa *Thin Solid Films* **153** 209 (1987)
176. Ch Taschner, A Leonhardt, M Schnoherr, E Wolf, J Henke *Mater. Sci. Eng.* **A139** 67 (1991)

177. X-M He, W-Zh Li, H-D Li *J. Mater. Res.* **9** 2355 (1994)
178. H Holleck, M Lahres *Mater. Sci. Eng.* **A140** 609 (1991)
179. A K Dua, V C George *Thin Solid Films* **247** 34 (1994)
180. P K Srivastava, V D Vankar, K L Chopra *Thin Solid Films* **161** 107 (1988)
181. A Cavaleiro, M T Vieira *Surf. Eng.* **10** 147 (1994)
182. H Holleck, H Schulz *Surf. Coat. Technol.* **36** 707 (1988)
183. C Mitterer, M Rauter, P Rodhammer *Surf. Coat. Technol.* **41** 351 (1990)
184. W Herr, B Matthes, E Broszeit, K H Kloos *Mater. Sci. Eng.* **A140** 616 (1991)
185. O Knotek, F Loffler *J. Hard Mater.* **3** 29 (1992)
186. J P Riviere, Ph Guesdon, J Delafond, M F Denanot *J. Less-Common Met.* **145** 477 (1988)
187. C Mitterer, A Ubleis, R Ebner *Mater. Sci. Eng.* **A140** 670 (1991)
188. P Hammer, A,Steiner, R Villa, M Baker, P N Gibson, J Haupt, W Gissler *Surf. Coat. Techn.* **68**/**69** 194 (1994)
189. R A Andrievskii, I A Belokon', V V Kapsheninov, V P Makarov, Z Kh Fuksman, G B Shvets *Izv. Akad. Nauk Kirg. SSR, Ser. Fiz.-Tekh. Mat.* (2) 32 (1989)
190. R A Andrievskii, I A Belokon', Z Kh Fuksman, in *High Performance Ceramic Films and Coatings* (Ed. P Vincenzini) (Amsterdam: Elsevier, 1991) p. 469
191. K Miura, I Ishigami, M Kuno, H Kaneda *J. Jpn. Inst. Met.* **59** 303 (1995)
192. Y W Bae, W Y Lee, T M Besmann, P J Blau *Appl. Phys. Lett.* **66** 1895 (1995)
193. B A Movchan, A V Demchishin, G F Badilenko, R F Bunshah, C Sans, C Deshpandey, H J Doerr *Thin Solid Films* **97** 215 (1982)
194. G Hilz, H Holleck *Int. J. Refract. Met. Hard Mat.* **14** 97 (1996)
195. R A Andrievskii *Int. J. Refract. Met. Hard Mat.* **14** 105 (1996)
196. S Veprek, S Reiprich, L Shizhi *Appl. Phys. Lett.* **66** 2640 (1996)
197. D Li, X Chu, Sh-C Cheng, X-W Lin, V P Dravid, Y-W Chung, M-Sh Wong, W D Sproul *Appl. Phys. Lett.* **67** 203 (1995)
198. D T Quinto *Int. J. Refract. Met. Hard Mat.* **14** 7 (1996)
199. D T Quinto, G J Wolfe, P C Jindal *Thin Solid Films* **153** 19 (1987)
200. R Kh Saidakhmedov, M G Karpman, G P Fetisov *Metalloved. Term. Obrab. Met.* (9) 8 (1993)
201. Y Sun, A Bloyce, T Bell *Thin Solid Films* **271** 122 (1995)
202. T Torok, A J Perry, L Chollet, W D Sproul *Thin Solid Films* **153** 37 (1987)
203. A J Perry *Thin Solid Films* **193** 463 (1990)
204. D S Stone, K B Yoder, W D Sproul *J. Vac. Sci. Technol.* **A9** 2543 (1991)
205. X Jiang, M Wang, K Schmidt, E Dunlop, J Haupt, W Gissler *J. Appl Phys.* **69** 3053 (1991)
206. P B Mikarimi, M Shinn, S Barnett, S Kumar, M Grimsditch *J. Appl. Phys.* **71** 4955 (1992)
207. E Vancoille, J P Celis, J R Roos *Thin Solid Films* **224** 168 (1993)
208. K I Portnoi, A A Mukaseev, V N Gribkov, Yu V Levinskii *Poroshk. Metall.* (5) 87 (1968)
209. P B Mikarimi, S A Barnett, K M Hubbard, T R Jervis, L Hultman *J. Mater. Res.* **9** 1456 (1994)
210. B Matthes, E Broszeit, K H Kloos *Surf. Coat. Technol.* **57** 97 (1993)
211. I Milosev, B Navinsek *Surf. Coat. Technol.* **63** 173 (1994)
212. I Yu Konyashin *Thin Solid Films* **249** 174 (1994)
213. K Holmberg, A Matthews *Coatings Tribology. Properties, Techniques and Application in Surface Engineering* (Amsterdam: Elsevier, 1994)
214. V P Bukatov, B M Ginzburg, Yu P Kozyrev, V A Krasnyi, V G Kuznetsov, E B Sedakova *Tren. Iznos* **15b** 1009 (1994)
215. Yu A Andreev, A N Shvaiko, E A Levashov, V I Kosyanin *Korroz. Met.* **31** 131 (1995)
216. H Holleck *Surf. Coat. Technol.* **36** 151 (1988)
217. M Ostling, S Nygren, C S Petersson, H Norstrom, R Buchta, H-O Blom, S Berg *Thin Solid Films* **145** 81 (1986)
218. D-Y Shih, C-A Chang, J Paraszczak, S Nunes, J Cataldo *J. Appl. Phys.* **70** 3052 (1991)
219. K Papathanassopoulos, W Wenzl *J. Phys. F Met. Phys.* **12** 1369 (1982)
220. E M Salomons, F Feenstra, D G Groot, J H Rector, R Griessen *J. Less-Common Met.* **130** 415 (1987)
221. R A Andrievskii, I A Anisimova, V P Anisimov *Neorg. Mater.* **28** 365 (1992)[c]
222. F Gorbilleau, R Hillel, G Nouet *Nanostruct. Mater.* **4** 215 (1994)
223. R A Andrievskii, I A Anisimova, V P Anisimov, V P Makarov, V P Popova *Thin Solid Films* **261** 83 (1995)
224. J G Chen *Chem. Rev.* **96** 1477 (1996)
225. V M Ievlev *Struktura Poverkhnostei Razdela v Plenkakh Metallov* (The Structure of Interfaces in Metallic Films) (Moscow: Metallurgiya, 1992)

[a] — *Russ. Phys. Solid. State (Engl. Transl.)*
[b] — *Russ. Phys. Tech. Phys. (Engl. Transl.)*
[c] — *Inorg. Mater. (Engl. Transl.)*
[d] — *Russ. Phys. JETP (Engl. Transl.)*